AN INFRARED STUDY OF CRYSTALLINE

STRONTIUM FORMATE AND

STRONTIUM FORMATE DIHYDRATE

by

NEIL ROBERT MCQUAKER

B.Sc., University of British Columbia, 1965

A THESIS SUBMITTED IN PARTIAL FUFILMENT OF

THE REQUIREMENTS FOR THE DEGREE OF

MASTER OF SCIENCE

in the Department of

CHEMISTRY

We accept this thesis as conforming to the

required standard

September, 1966

UNIVERSITY OF BRITISH COLUMBIA

## ABSTRACT

The infrared absorption spectra of single crystals of strontium formate and strontium formate dihydrate have been recorded between 4000 and 500 cm$^{-1}$. Crystal slices cut perpendicular to the crystal axes were employed; the spectra were recorded using polarized radiation, the electric vector being parallel to the direction defined by the crystal axis in question.

For $Sr(CHO_2)_2$ it was possible to assign 20 of the 36 infrared active internal fundamentals. In addition lattice modes at: 10, 12, 15, 20, 23, 70, 155, 180 and 200 cm$^{-1}$ were infered from combinations with internal fundamentals.

For $Sr(CHO_2)_2 \cdot 2H_2O$ it was possible to observe only 10 of the 36 internal fundamentals associated with the formate ions as the absorbing species. Of the 18 internal fundamentals associated with the water molecules as the absorbing species only one mode could be unambiguously assigned. Lattice modes at: 642, 710, 750, 797, 840, 856 and 872 cm$^{-1}$ were observed and two additional lattice modes at 18 and 110 cm$^{-1}$ were infered from combinations with internal fundamentals.

From the intensity ratios of the internal fundamentals of $Sr(CHO_2)_2$ it was possible to calculate the direction cosines associated with each of the two crystallographically non-equivalent formate ions contained in the unit cell.

## ACKNOWLEDGEMENT

TABLE OF CONTENTS

# LIST OF TABLES

## LIST OF FIGURES

CHAPTER I    INTRODUCTION

## 1-1   Introductory Remarks

The vibrational spectra of $Sr(CHO_2)_2$ and $Sr(CHO_2)_2 \cdot 2H_2O$ have been the subject of investigation of previous workers (1-5). Only in the study of $Sr(CHO_2)_2 \cdot 2H_2O$ (4,5) were single crystals and polarized radiation used.

In this work spectra of polycrystalline strontium formate and strontium formate $d_1$ were studied as well as single crystal spectra of both $Sr(CHO_2)_2$ and $Sr(CHO_2)_2 \cdot 2H_2O$.

The single crystal spectra were studied using polarized infrared radiation as a continuation of the study of inorganic formates initiated in this laboratory by B.A. Morrow (6) and subsequently continued by T.L. Charlton (7).

As will be discussed later it is necessary when considering the spectra of single crystals to take account of the orientation of the absorbing species with respect to the crystal axes. This orientation of the absorbing species with respect to the crystal axes is directly related to the intensity of the internal fundamental modes of

vibration associated with the absorbing species. Consequently information obtained from polarized spectra of single crystals is not only an aid in making vibrational assignments but can also aid in the determination of crystal structures-particularly where hydrogen atoms are involved.

## 1-2 The Crystal Structure of $Sr(CHO_2)_2$

The crystal structure of $Sr(CHO_2)_2$ is described by Nitta and his co-workers (8-10) as being orthorhombic and belonging to the space group $P2_12_12_1(D_2^4)$. The cell parameters and the co-ordinates of the generating atomic positions are listed in Table 1-1 (i). The hydrogen atom positions were calculated by the author on the assumption of a value of 1.09 $A^O$ for the C-H bond length. The formate ion parameters were also calculated and are given in Table 1-1 (ii).

The crystal structure of $Sr(CHO_2)_2$ can be visualized from the projection on to the (001) plane given in Fig. 1-1. We see that the structure maybe described as consisting of complex chains along the screw parallel to the C axis; the chains being linked laterally through the oxygen atoms of the formate ions.

## 1-3 The Crystal Structure of $Sr(CHO_2)_2.2H_2O$

A preliminary X-ray analysis of $Sr(CHO_2)_2.2H_2O$ was reported by Nitta in 1928 (8) with subsequent work being done by Osaki (9). It was found that the dihydrate like anhydrous strontium formate belongs to the space group $P2_12_12_1(D_2^4)$. The cell parameters and the co-ordinates of the generating atomic positions as given by Osaki are listed in Table 1-2 (i). Again the hydrogen atom positions were

calculated by the author, a value of 1.09 $A^{o}$ being assumed for the C-H bond length. The formate ion parameters are given in Table 1-2 (ii).

Fig. 1-2 shows a projection of the structure onto the (OO1) plane. The structure is similar to that of $Sr(CHO_2)_2$ and also maybe described as consisting of complex chains along the screw axis parallel to the C axis, with the chains being linked laterally through the water molecules and the oxygens of the formate ions.

TABLE 1 - 1

CRYSTAL STRUCTURE OF $Sr(CHO_2)_2$

Space Group: $P2_12_12_1$ $(D_2^4)$

a = 6.874 A°        b = 8.748 A°        c = 7.267 A°

(i) Generating Positions with Origin Halfway Between Three Pairs of Non Intersecting Screw Axes:

4 $Sr^{2+}$ Ions at (0.2500, 0.0915, 0.0000)

FORMATE ION I

4 O  atoms at  (0.005, 0.260, 0.420)
4 H  atoms at  (0.046, 0.298, 0.558) *
4 O  atoms at  (0.105, 0.154, 0.358)
4 O' atoms at  (-0.134, 0.330, 0.350)

FORMATE ION II

4 C  atoms at  (0.118, 0.303, 0.906)
4 H  atoms at  (0.255, 0.301, 0.831) *
4 O  atoms at  (-0.018, 0.235, 0.828)
4 O' atoms at  (0.120, 0.370, 1.057)

(ii) Formate Ion Parameters:

FORMATE ION I

$\underline{r}(C-O)$ = 1.24A°        $\underline{r}(C-O')$ = 1.24A°
$\underline{r}(C-H)$ = 1.09A°        $\angle(O-C-O')$ = 130°

FORMATE ION II

$\underline{r}(C-O)$ = 1.24A°        $\underline{r}(C-O')$ = 1.24A°
$\underline{r}(C-H)$ = 1.09A°        $\angle(O-C-O')$ = 129°

* Assuming $\underline{r}(C-H)$ = 1.09 A° as Indicated in (ii)

TABLE 1 - 2

## CRYSTAL STRUCTURE OF $Sr(CHO_2)_2 \cdot 2H_2O$

Space Group: $P2_12_12_1$ $(D_2^4)$

$a = 7.332$ A°    $b = 12.040$ A°    $c = 7.144$ A°

(i)  Generating Positions with Origin Halfway Between Three Pairs of Non Intersecting Screw Axes:

4 $H_2O_I$ Molecules at   (0.411, 0.092, -0.469)

4 $H_2O_{II}$ Molecules at (-0.025, 0.221, 0.241)

4 $Sr^{2+}$ Ions     at (0.2500, 0.0715, 0.1970)

### FORMATE ION I

4 C  atoms at   (0.020, 0.186, -0.223)
4 H  atoms at   (0.009, 0.183, -0.375) *
4 O  atoms at   (0.112, 0.116, -0.147)
4 O' atoms at   (-0.061, 0.259, -0.144)

### FORMATE ION II

4 C  atoms at   (-0.142, -0.012, 0.417)
4 H  atoms at   (-0.201, -0.095, 0.429)*
4 O  atoms at   (0.022, -0.005, 0.450)
4 O' atoms at   (-0.247, 0.063, 0.372)

(ii)  Formate Ion Parameters:

### FORMATE ION I

$\underline{r}(C-O) = 1.21$A°    $\underline{r}(C-O') = 1.20$A°
$\underline{r}(C-H) = 1.09$A°    $\angle(O-C-O') = 125°$

### FORMATE ION II

$\underline{r}(C-O) = 1.23$A°    $\underline{r}(C-O') = 1.23$A°
$\underline{r}(C-H) = 1.09$A°    $\angle(O-C-O') = 128°$

*  Assuming $\underline{r}(C-H) = 1.09$ A° as Indicated in (ii)

# FIG 1·1   CRYSTAL STRUCTURE OF Sr(CHO$_2$)$_2$

## (i) Projection of Structure on (OO1)
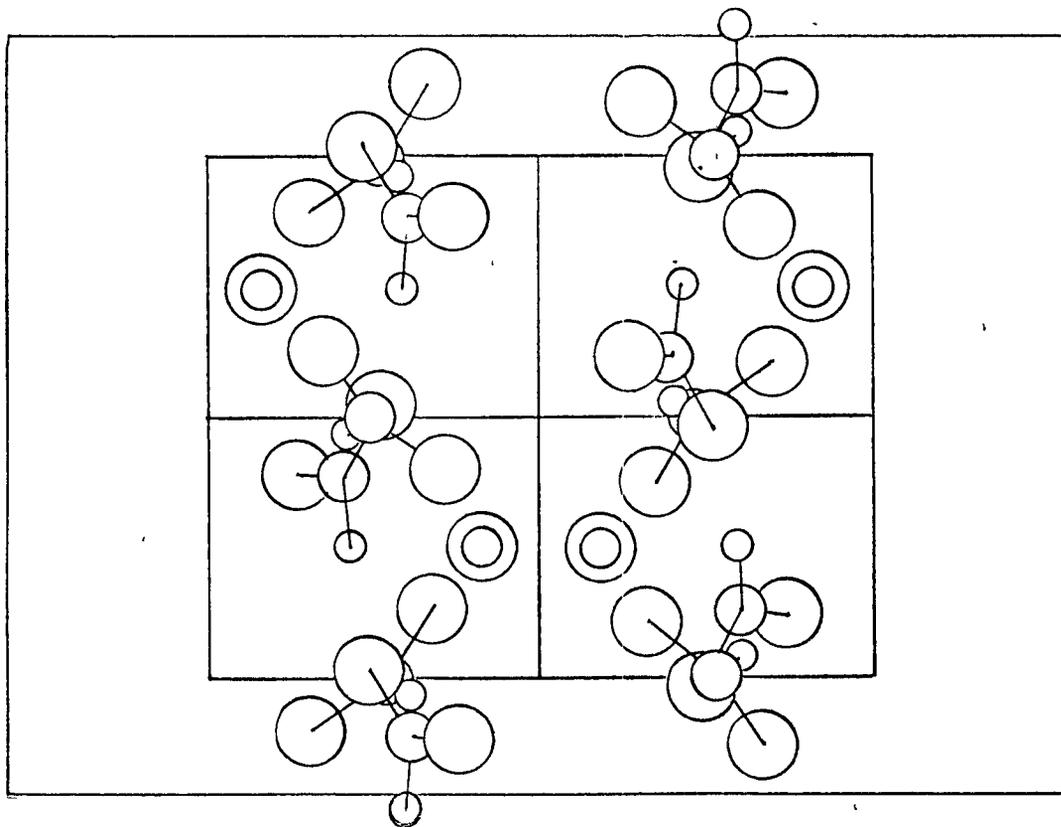


## (ii) Symmetry Elements of the Unit Cell

# FIG 1-2  CRYSTAL STRUCTURE OF $Sr(CHO_2)_2 \cdot 2H_2O$

## (i) Projection of Structure on (001)
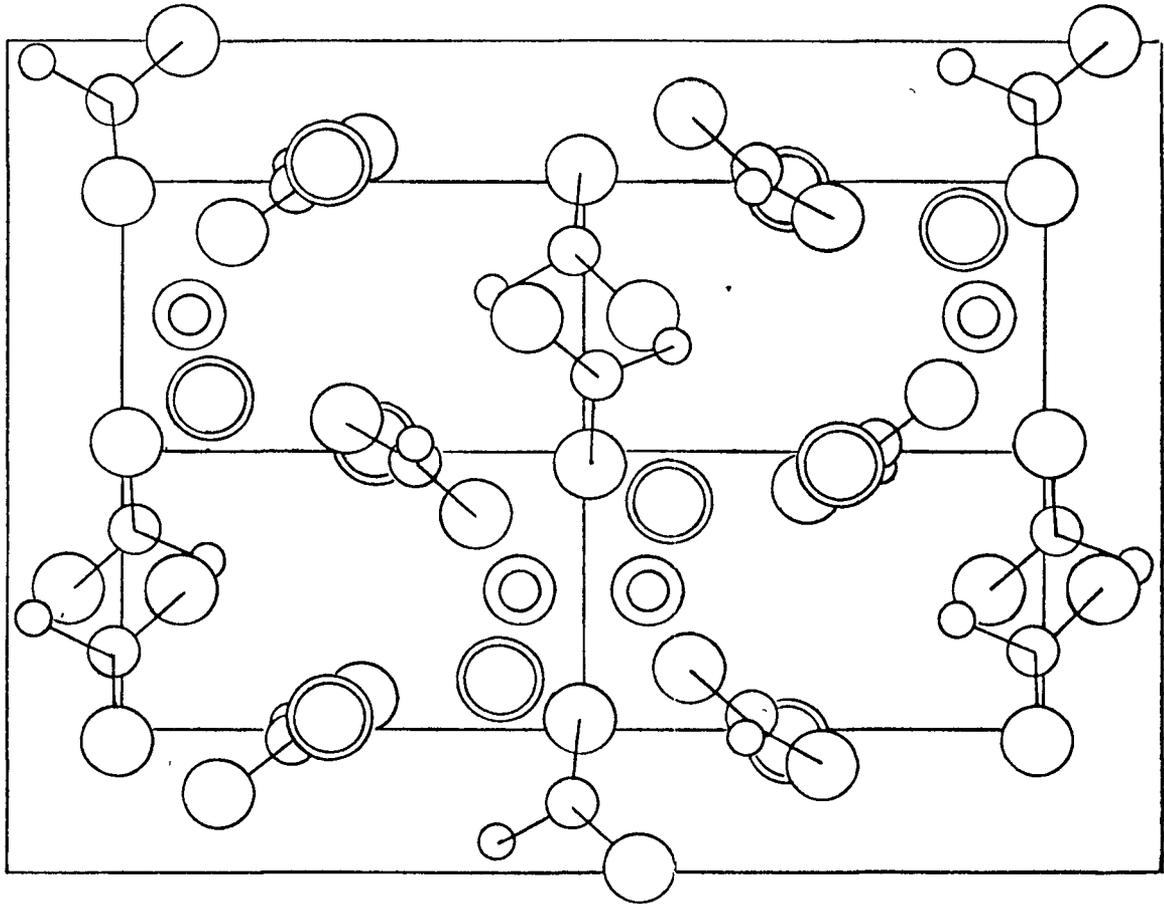


## (ii) Symmetry Elements of the Unit Cell
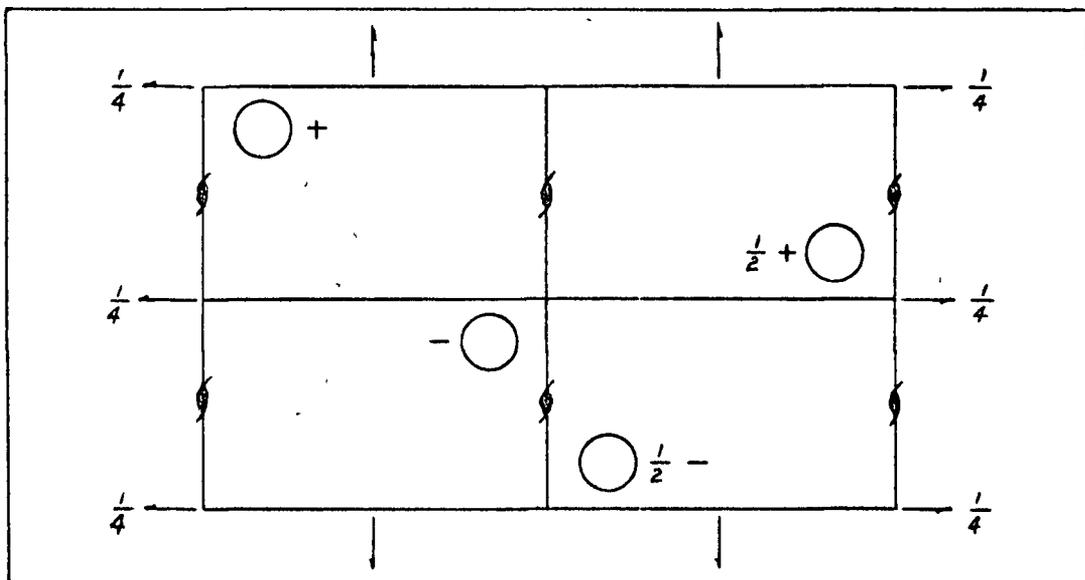
## CHAPTER II    EXPERIMENTAL

### 2-1  Materials

The strontium formate used was prepared by neutralization of formic acid with strontium carbonate.  The product was filtered and recrystallized from solution.  Both the strontium carbonate and formic acid were of reagent grade and were obtained from the British Drug Houses Ltd.

The strontium formate $d_1$ was prepared in a similar manner using formic acid- $d_1$.

### 2-2  Growth of Single Crystals

The crystals were grown from aqueous solution by slow evaporation at constant temperature; the hydrated crystals being grown at $60^{\circ}C$ and the anhydrous at $85^{\circ}C$.

Crystal growth was carried out in liter vacuum flasks; the following procedure was followed.  Initially a liter of nearly saturated solution was prepared at the growing temperature, care being taken that there were no impurities in the solution.  The solution was then maintained at the growing temperature and allowed to evaporate slowly- slow evaporation was achieved by placing a cotton plug in the mouth of the flask.  The flask was watched carefully so

that the first sign of seed crystals forming on the bottom
of the flask could be detected. When this occurred one
of two procedures was followed depending on whether a harvest
of seed crystals was desired or whether it was desired to
start the growth of a large single crystal.

If seeds were desired the slow evaporation was continued
until they had reached a size of about 3-5 mm. in length.
They were then harvested.

If it was desired to grow a single crystal a seed
crystal was placed in the saturated solution suspended by
a thin nylon filament. The free end of the nylon filament
was secured on the arm projecting from the vacuum flask.
This process was carried out in minimumal time so that as
little vapour as possible escaped from the flask.

After sufficient growth had taken place (usually after
a period of about 3-4 weeks) the crystal was removed from
the saturated solution. However, when removing the crystals
from the saturated solution it was found that the thermal
strain imposed by the sudden change in temperature was
sufficient to severely crack the crystal. In order to
circumvent this problem Nujol at the temperature of the
saturated solution was placed on top of the saturated solution.
The crystal was then drawn up into the Nujol layer and the
temperature lowered to room temperature over a period of

about 8 hours.  The crystals so obtained were largely free
from cracks and internal flaws.

Both the hydrated and anhydrous crystals when grown
in the above manner were of sphenoidal habit, 10 to 15 mm.
wide, 20 to 30 mm. long and 7 to 10 mm. thick.  The principal
face of both crystals was the (010) face elongated in the
$\underline{C}$ direction.

## 2-3   Sample Preparation

The most difficult part of the experimental work was
preparing spectroscopically thin crystal slices (i.e. 20-30μ)
from the single crystal.  The following technique was
developed during the course of the experimental work.

The single crystal was first mounted with epoxy resin
(Aradite Adhesive, Ciba Ltd.), on a specially designed
support, care being taken that the desired crystal axis was
mounted perpendicular to the base of the support.  The
crystal and its support were then mounted in a crystal
cutting device so that the desired crystal axis was per-
pendicular to the cutting plane.

The cutting plane consists of a 3 by 6 inch table with
rollers at either end.  In the centre of this table there is
a $1\frac{1}{2}$ inch circular opening below which is the crystal
support.  Provision is made to elevate, rotate and tilt this

support so that the crystal maybe appropriately positioned with respect to the cutting plane.

Once the crystal was appropriately mounted in the crystal cutter, cutting began. In order to cut the crystal a piece of No. 40 cotton thread was held against the crystal and pulled back and forth across the rollers at either end of the cutting table. A carborundum-water slurry was placed on the cutting table to act both as a lubricant and as an aid to the cutting process. Using this method it was possible to cut a cross section of 600 mm.$^2$ in about one-half hour.

After the crystal was cut the face of the portion of the crystal remaining on the crystal support was polished. This polishing process was carried out in two steps. The first step made use of a polishing disc. The surface of this disc was covered with No. 360-A carborundum paper and it was mounted so that it rotated horizontally at about 3000 R.P.M. The crystal face to be polished was held against the rotating disc; care being taken to rotate the crystal at evenly spaced intervals so as to ensure as flat a surface as possible.

Once a flat uniformly smooth surface had been obtained the second step in the polishing process was carried out. This process, which brought the crystal face to an extremely high polish, consisted of rubbing the crystal face on a piece of velvet lap stretched over a flat glass plate;

dampened jewellers rouge being used as the polishing compound.

After the crystal face had been satisfactorily polished the crystal face was coated with silver paint (Silver Print; G.C. Electronics Co.) except for an area of 3 x 11 mm., this area being the size of the slit on the sample holders. When the silver paint had dried the whole of the crystal face was covered with a coat of plastic cement (Radio Service Cement; General Cement Mfg. Co.). After the plastic cement had dried epoxy resin was used to glue a piece of glass plate measuring $\frac{1}{4}$ x $1\frac{1}{2}$ x $1\frac{1}{2}$ inches to the crystal face. Care was taken that no air bubbles were trapped under the small glass plate.

The purpose of the epoxy was to provide a firm backing for the crystal which contained no glue-free pockets. Such a backing was crucial once the final stages of polishing were reached. After the epoxy had been allowed to set the crystal was so positioned in the crystal cutter that a slice about 0.5 mm. thick could be cut. This slice which was mounted on the small glass plate was then ground on the polishing disc in the manner outlined previously. Where the crystal was coated with silver paint it was possible to measure the thickness of the crystal directly with a Zeiss Light Section Microscope as the polishing process progressed. It should be noted that the purpose of the plastic cement as will be mentioned later was to allow for the action of

acetone to free the crystal slice from the glass plate once
the polishing process was completed.

When the crystal slice reached a thickness of about
50 $\mu$ the 6 cm. polishing disc was replaced by a 7 mm. disc
and the polishing process continued until a thickness of
35-40 $\mu$ had been reached.  The final stage of polishing was
carried out by replacing the carborundum surface on the small
disc by a chamois surface well impregnated with jewellers
rouge- nujol being used as a lubricant.  It was found that
the crystal slice showed no tendency to crack or chip
during the polishing process.

After the crystal slice had been polished to the
desired thickness (about 25$\mu$) the glass plate supporting
the crystal was placed in a Petri dish and covered with a
bath of anhydrous acetone.  The Petri dish was then left
in a dessicator for about two hours which was sufficient
time for the acetone to dissolve the plastic cement and
enable the crystal slice to float free.

The next step in the sample preparation was transferring
the crystal slice to the sample holder.  (The sample holder
was simply a brass disc designed to fit the keys on the
spectrometer mounting so that the sample could be placed
as close as possible to the entrance slit).  In order to
transfer the crystal slice to the sample holder, the sample
holder was placed in the acetone bath and a fine hair brush

was used to gently position the crystal slice over the 3 x 11 mm. slit in the sample holder. The silver paint which still adhered to the crystal slice could be used as a convenient guide in aligning the crystal and the slit in the sample holder.

Once the crystal had been correctly positioned on the sample holder, the acetone was carefully removed from the Petri dish. Finally the crystal slice was glued sparingly at the edges to the sample holder. Plastic cement was used for this purpose. Now that the crystal was mounted a final measurement was made of the thickness of the crystal using the Zeiss Light Section Microscope. The thickness of the crystals used in this work were found to be of the order of 25 $\mu$. In most cases it was found that the surfaces of the crystal were not planar (i.e., over the 11 mm. length of the crystal exposed to the sample beam the crystal slice usually tapered from about 30 to 20 $\mu$).

In order to check the relative orientation of the crystal axes a Zeiss Polarizing Microscope was used. Observation of interference figures also made it possible to confirm that the crystals were ground to one or two degrees of the perpendicular.

## 2-4  Apparatus

The spectra were recorded in the region of 4000 to
500 cm$^{-1}$ using a Perkin Elmer 421 spectrometer with two dual
grating interchanges, the error of measurement being
estimated as $\pm$ 2 cm$^{-1}$ with a reproducibility of $\pm$ 1 cm$^{-1}$.
The polarizer constructed in the Mechanical shop, consisted
of two three-sheet stacks of 0.5 mm. silver chloride plates
mounted in the form of a V (12) to prevent displacement of
the spectrometer beam.  Measurements in the visible region
against a Wollaston prism indicate that less than 5% of the
component perpendicular to the desired component and the
beam is passed.  Measurements of the convergence of the
sample beam showed that less than 1% of the component
parallel to the beam direction would be introduced by the
convergence.

CHAPTER III    RESULTS

This Chapter contains reproductions
of spectra obtained during the course of
the experimental work.  For convenience
they are divided into three groups;
spectra of polycrystalline strontium
formate; single crystal spectra of $Sr(CHO_2)_2$
and single crystal spectra of $Sr(CHO_2)_2.2H_2O$.
The Chapter also contains Tables giving
vibrational assignments of the respective
groups of spectra.  Discussion of the basis
for the assignments is left until Chapters
V and VI.

## 3-1  Spectra of Polycrystalline Strontium Formate

The samples used to obtain the spectra in Fig. 2

were obtained using the thin film technique which consists

of mechanically depositing a thin film of the sample on an

appropriate support.  In this work KBr windows were used.

Vibrational assignments along with the results of previous

workers (1-3) are given in Table 2.

## 3-2  Single Crystal Spectra of $Sr(CHO_2)_2$ and $Sr(CHO_2)_2.2H_2O$

The samples used to obtain the spectra in Fig. 3 and

Fig. 4 were obtained using the techniques outlined in

section 2-3; as already indicated the samples were approx-

imately $25\mu$ thick.  The vibrational assignments for the

polarized single crystal spectra of $Sr(CHO_2)_2$ and

$Sr(CHO_2)_2 \cdot 2H_2O$ are given in Tables 3 and 4-1 respectively.
The results for single crystals of $Sr(CHO_2)_2 \cdot 2H_2O$ obtained
by Vierne (4,5) using infrared reflection techniques are
contained in Table 4-2; the assignments are his.

It should be noted that for the polarized single crystal
spectra the reference to polarization parallel (ll) to a
certain crystallographic axis refers to the electric vector
being parallel to the direction defined by the crystal axis.
In the tables and in subsequent discussion vibrational modes
will be referred to as X(a), Y(c) or Z(c) active; a, b and c
refering to the crystal axis to which the electric vector
is parallel.

For the polarized spectra of $Sr(CHO_2)_2$ in the 810-730
$cm^{-1}$ region (Fig. 3-4 and 3-5) the crystal face is noted on
the spectra. For the remainder of the polarized spectra
the observed spectra did not appear to be dependent upon
the crystal face.

FIG 2-1  SPECTRA  OF POLYCRYSTALLINE  STRONTIUM  FORMATE

(i)  Sr(CHO$_2$)$_2$    4000-500  cm$^{-1}$
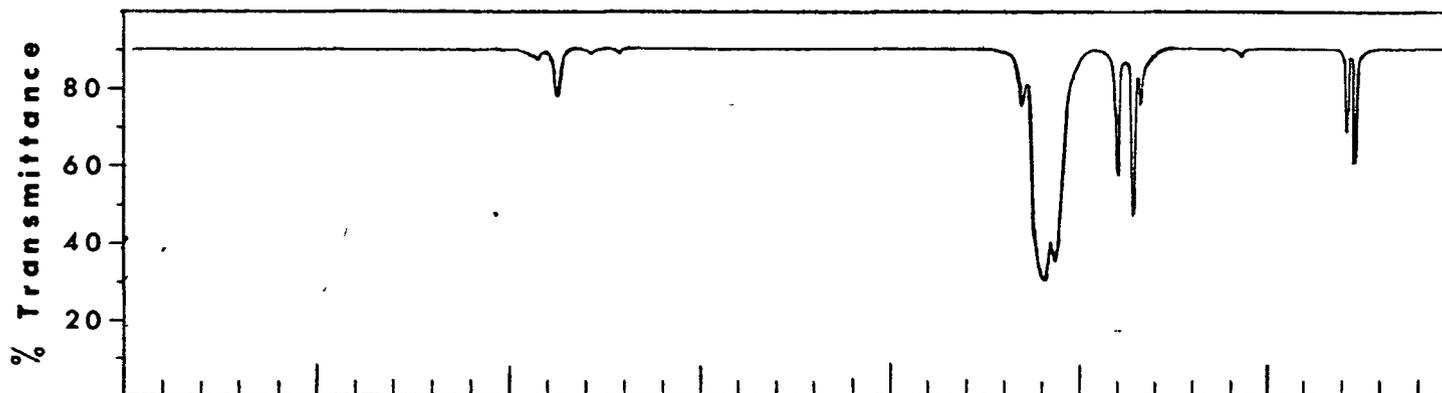
(ii)  Sr(CDO$_2$)$_2$   4000-500  cm$^{-1}$
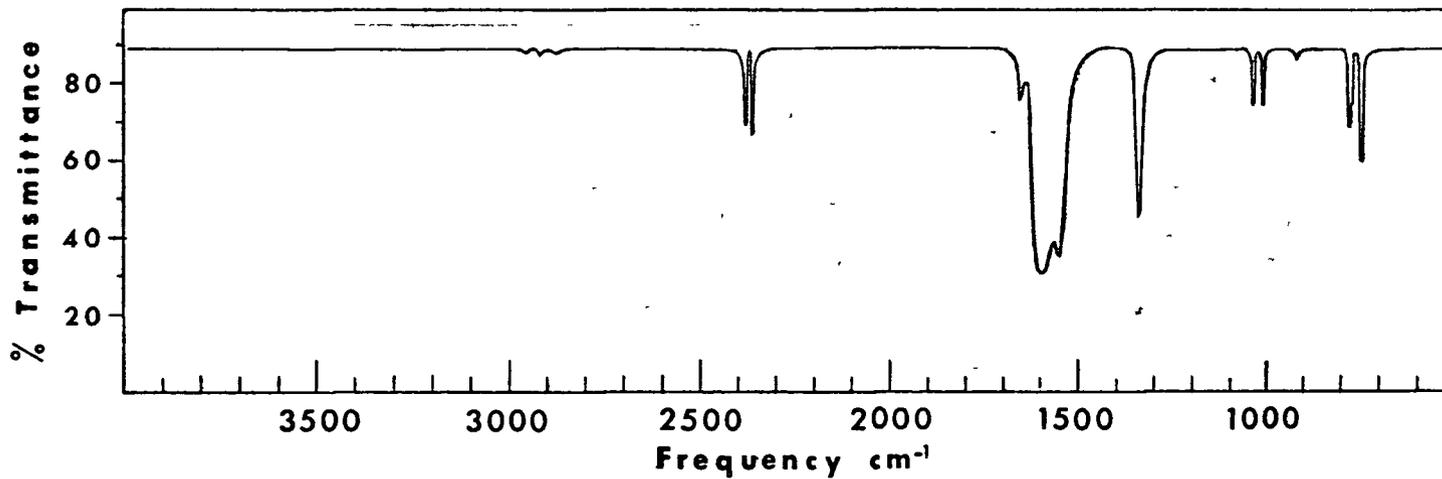
# FIG 2-2 SPECTRA OF POLYCRYSTALLINE STRONTIUM FORMATE

(i) $Sr(CHO_2)_2$ 1400-1320 cm$^{-1}$
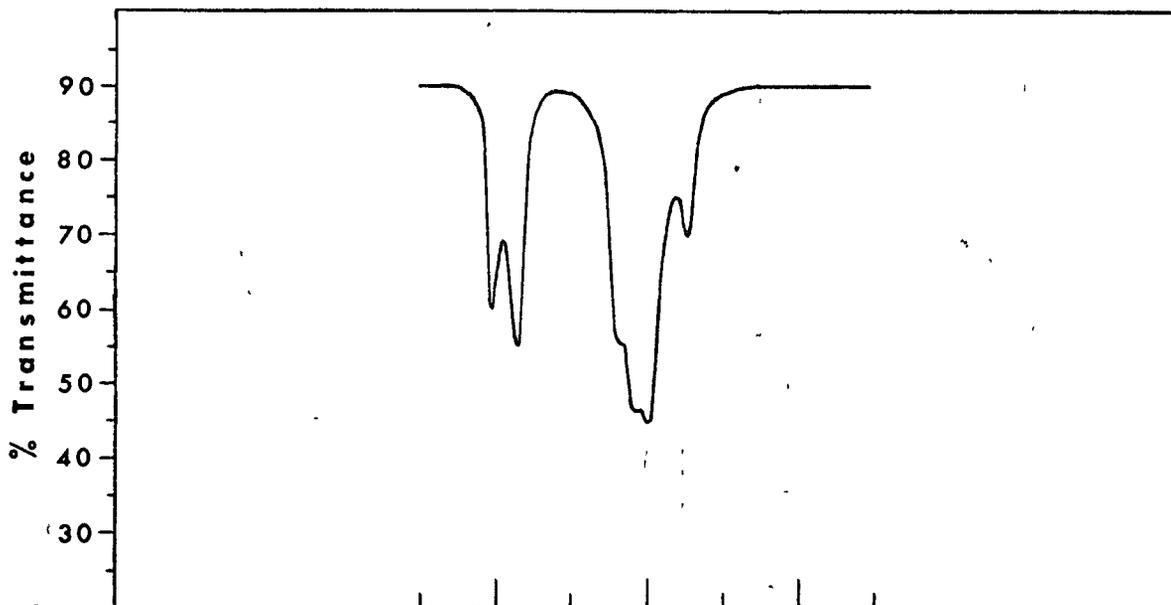


(ii) $Sr(CDO_2)_2$ 1400-1320 cm$^{-1}$
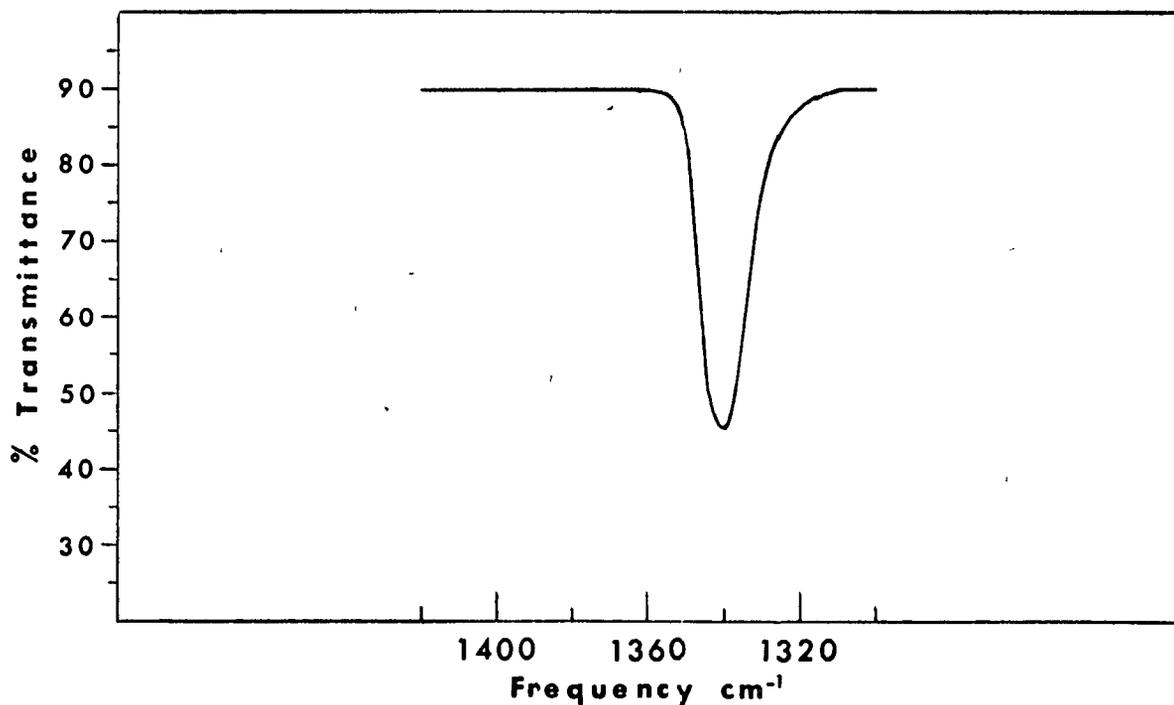
# FIG 2·3 SPECTRA OF POLYCRYSTALLINE STRONTIUM FORMATE

(i)   Sr(CHO$_2$)$_2$   810-730 cm$^{-1}$
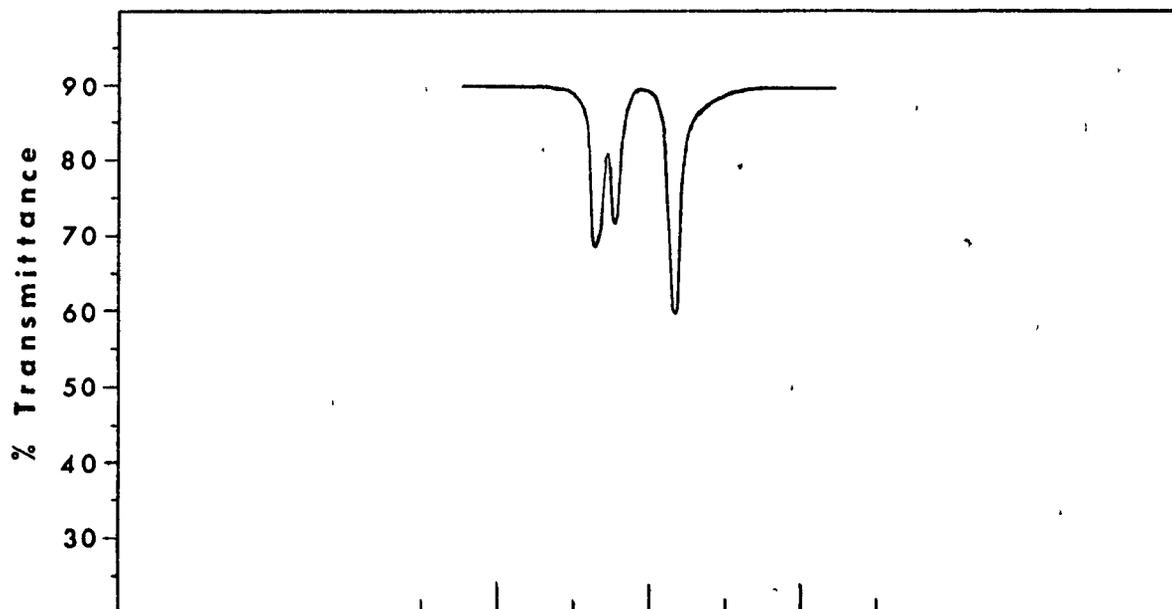


(ii)  Sr(CDO$_2$)$_2$   810-730 cm$^{-1}$



Frequency cm$^{-1}$
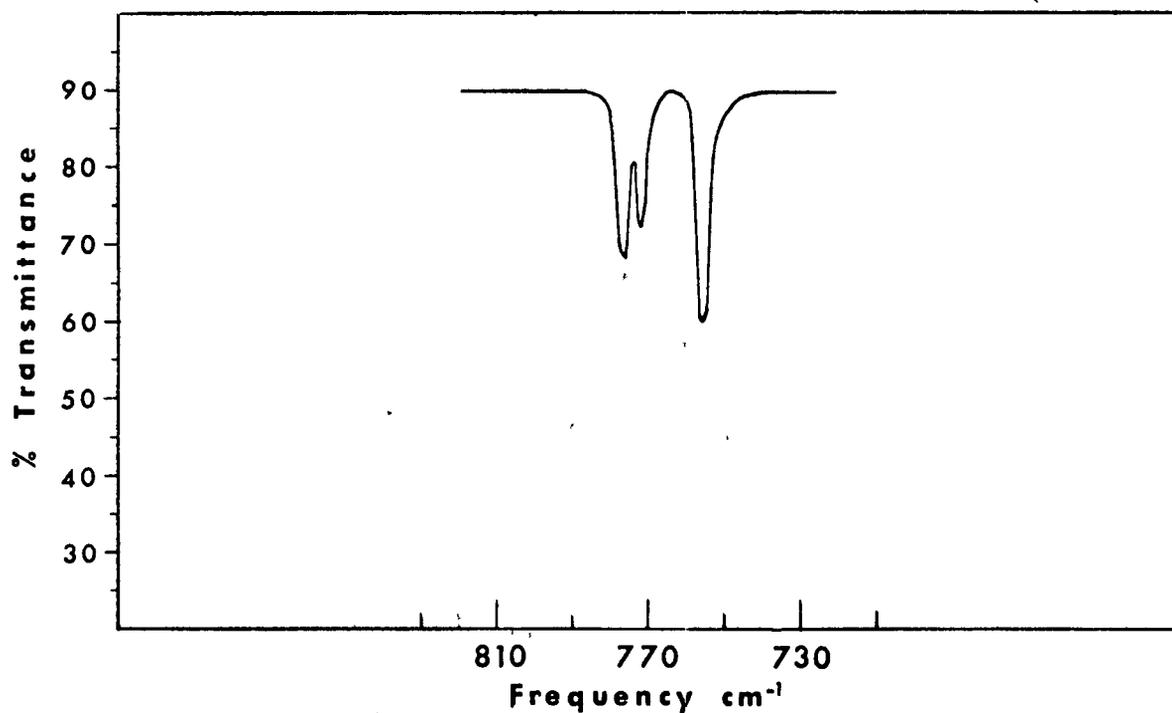
TABLE 2

### VIBRATIONAL ASSIGNMENTS FOR SPECTRA OF POLYCRYSTALLINE
### STRONTIUM FORMATE (WAVENUMBERS IN $CM^{-1}$)

| Mode | Harvey et al | Schutte and Buijs | Donaldson et al | $Sr(CHO_2)_2$ This Work | $Sr(CDO_2)_2$ This Work |
|---|---|---|---|---|---|
| $\nu_3(\delta OCO)a_1$ | 763 780 784 | 765 781 785 | 763 781 786 | 763 779.5 783.5 | 755 772 776 |
| $\nu_6(\rho CH)b_2$ | 1070 1082 | 1085 | 1087 | 1084 | 919 |
| | 1350 | | 1351 | 1349 | |
| $\nu_2(\nu CO)a_1$ | 1360 1369 | 1362 1374 | 1364 1374 | 1359.5 1362.5 1368 | 1340 |
| $\nu_5(\omega CH)b_1$ | 1381 1387.5 | 1397 1401 | 1399 1404 | 1393.5 1399 | 1013 1039 |
| $\nu_4(\nu CO)b_1$ | 1580 | 1572 1590 | 1572 | 1570 1593 | 1562 1593 |
| | | 1653 | | 1651 | 1650 |
| | 2720 2775 | | | 2720 2775 | |
| $\nu_1(\nu CH)a_1$ | 2872 | 2849 | 2874 | 2872 | 2160 2183 |
| | 2925 | | | 2925 | |

# FIG 3-1 POLARIZED SPECTRA OF $Sr(CHO_2)_2$ 3300-2600 cm$^{-1}$
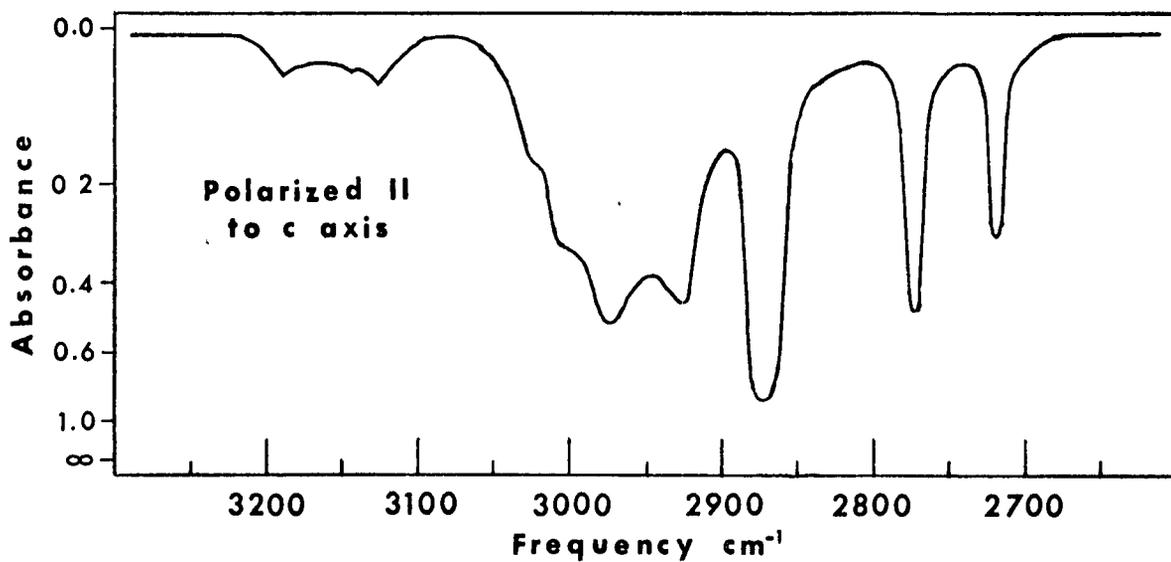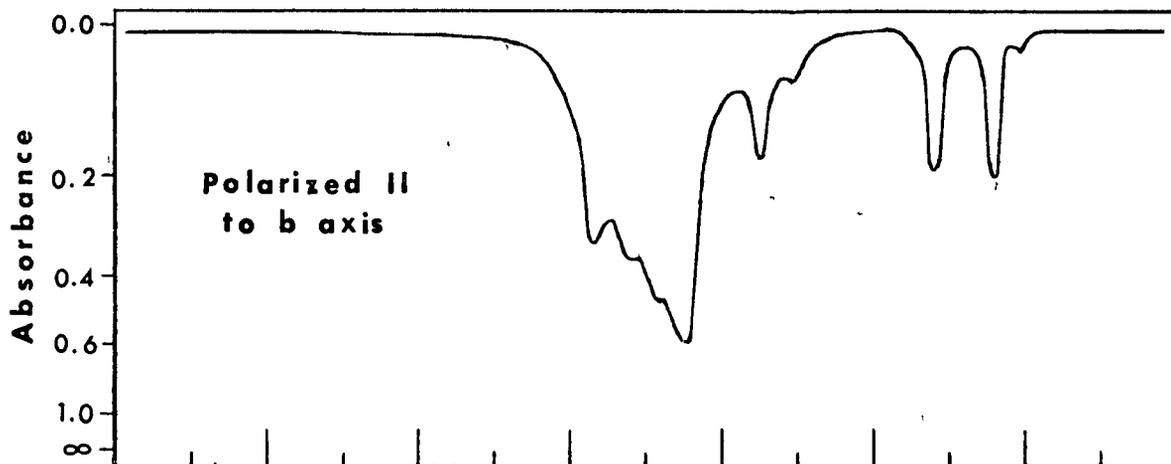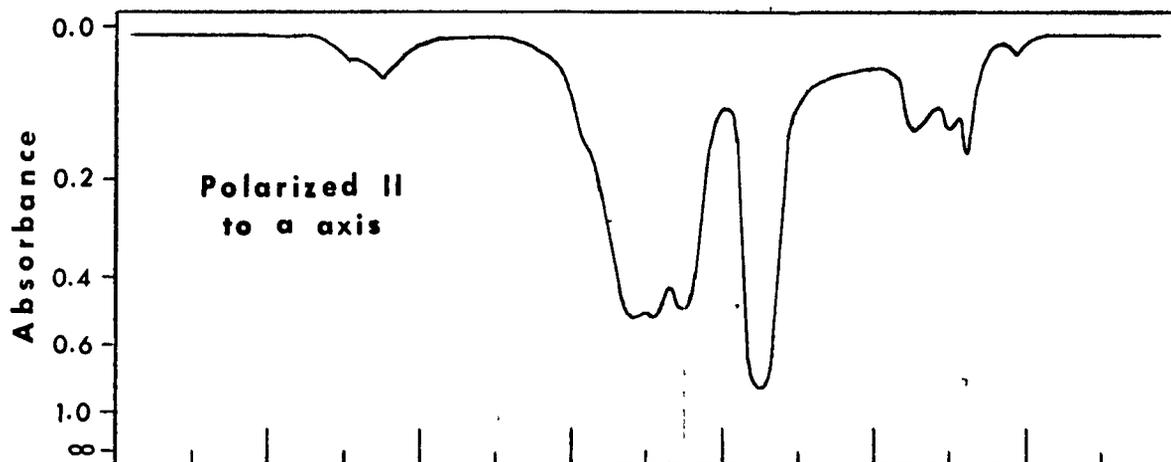
# FIG 3-2 POLARIZED SPECTRA OF Sr(CHO₂)₂ , 2000-1200 cm⁻¹
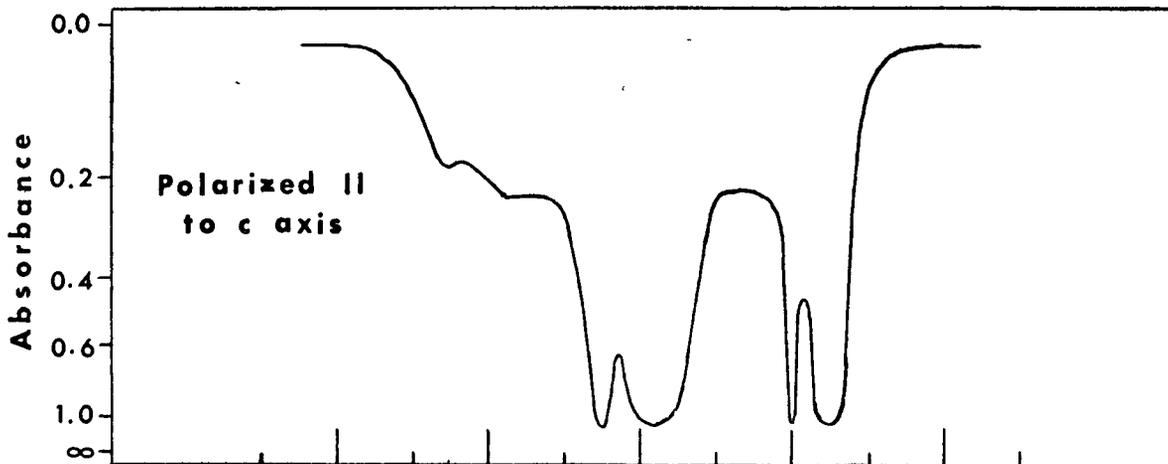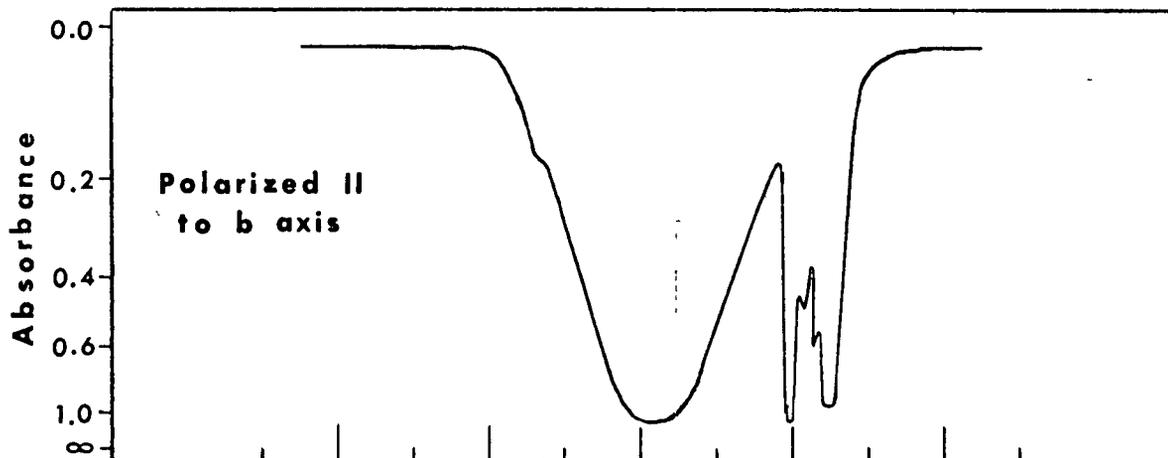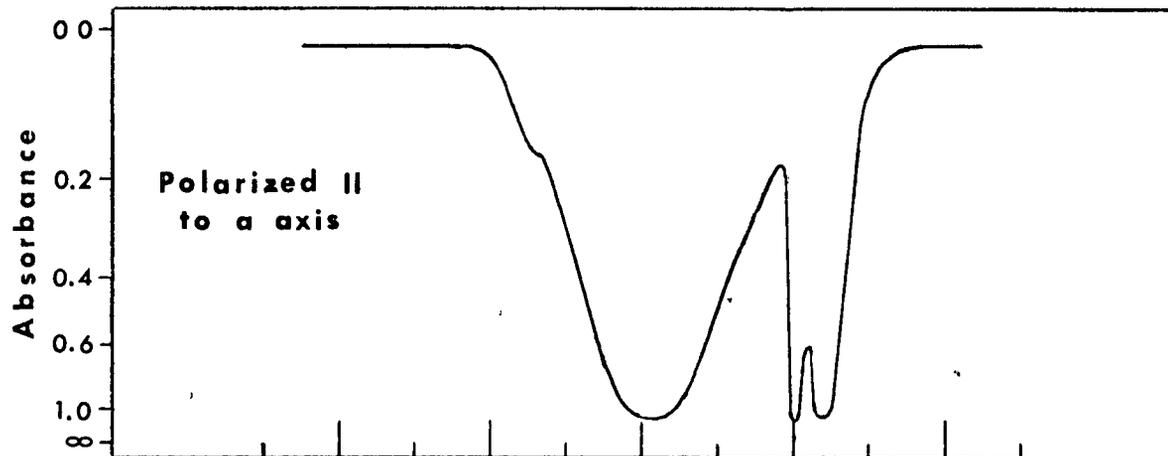


FIG 3-2 POLARIZED SPECTRA OF $Sr(CHO_2)_2$ , 2000-1200 $cm^{-1}$

# FIG 3-3 POLARIZED SPECTRA OF Sr(CHO₂)₂   1120-1040   cm⁻¹
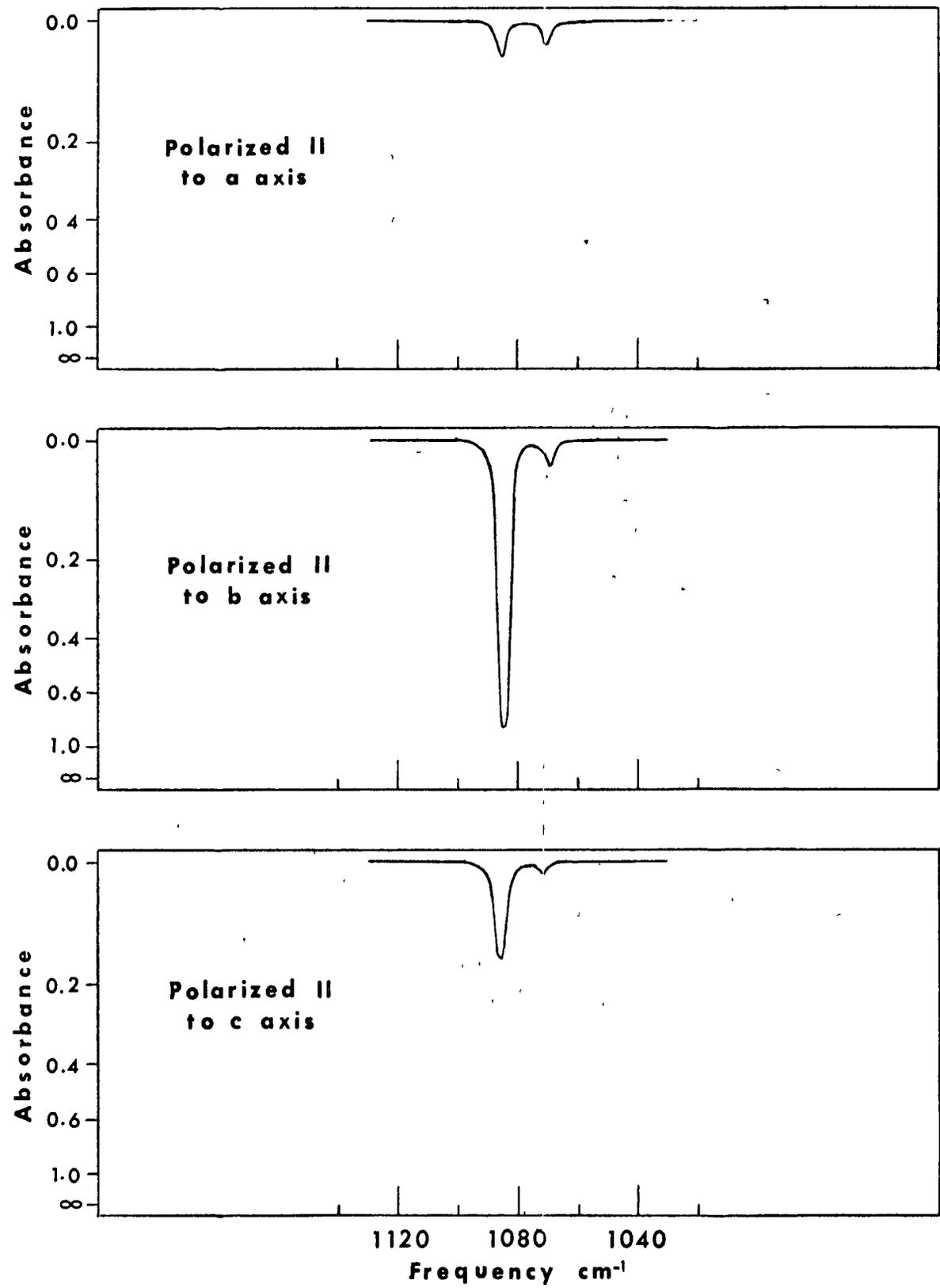
# FIG 3-4 POLARIZED SPECTRA OF Sr(CHO$_2$)$_2$    810-730 cm$^{-1}$

# FIG 3-5 POLARIZED SPECTRA OF $Sr(CHO_2)_2$    810-730 cm$^{-1}$



Polarized ‖ to a axis ac face

Polarized ‖ to b axis bc face

Polarized ‖ to c axis bc face
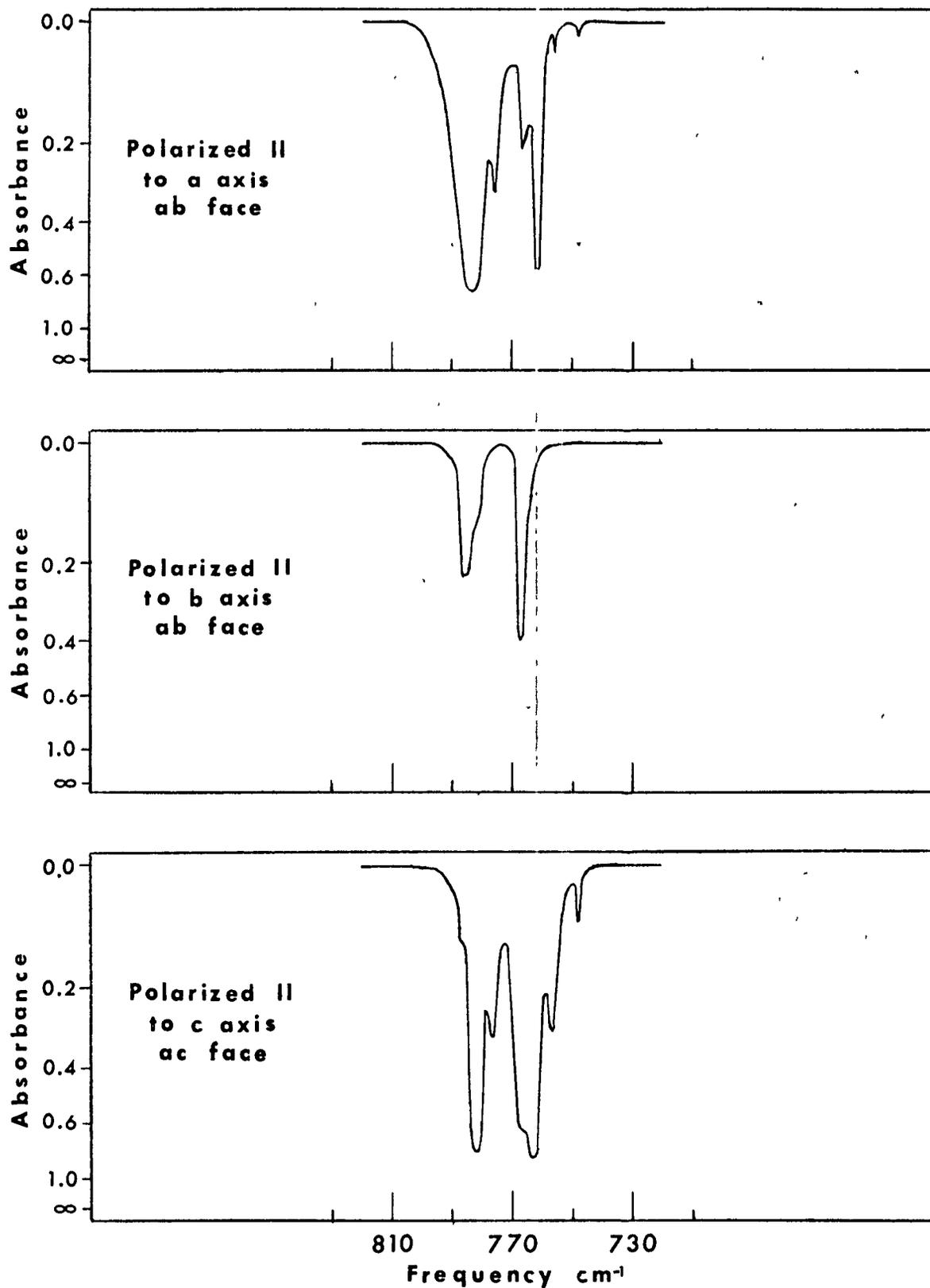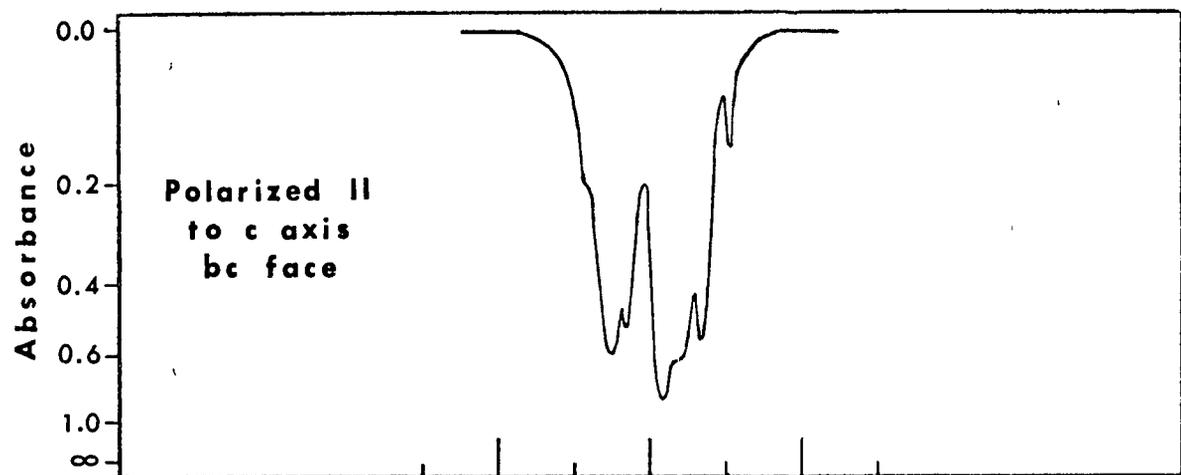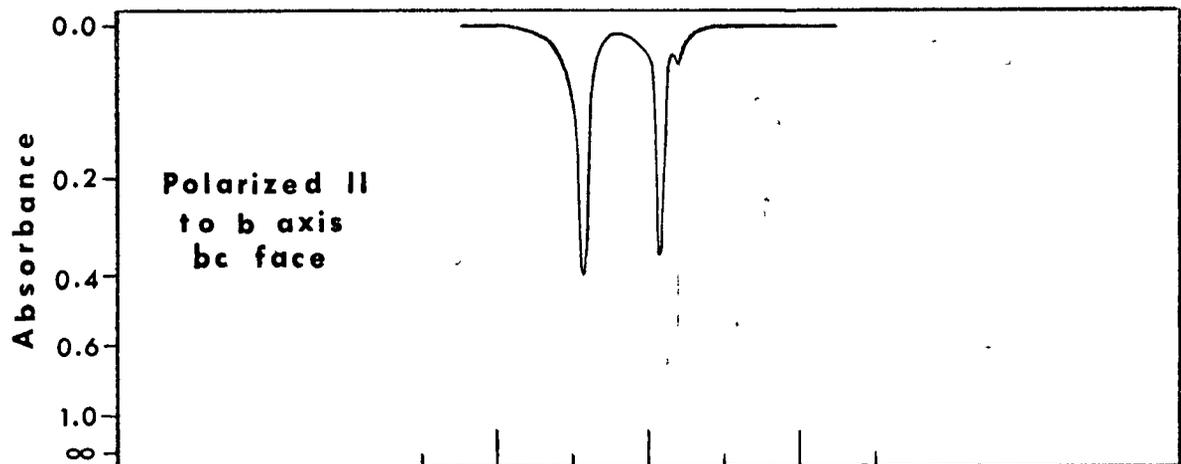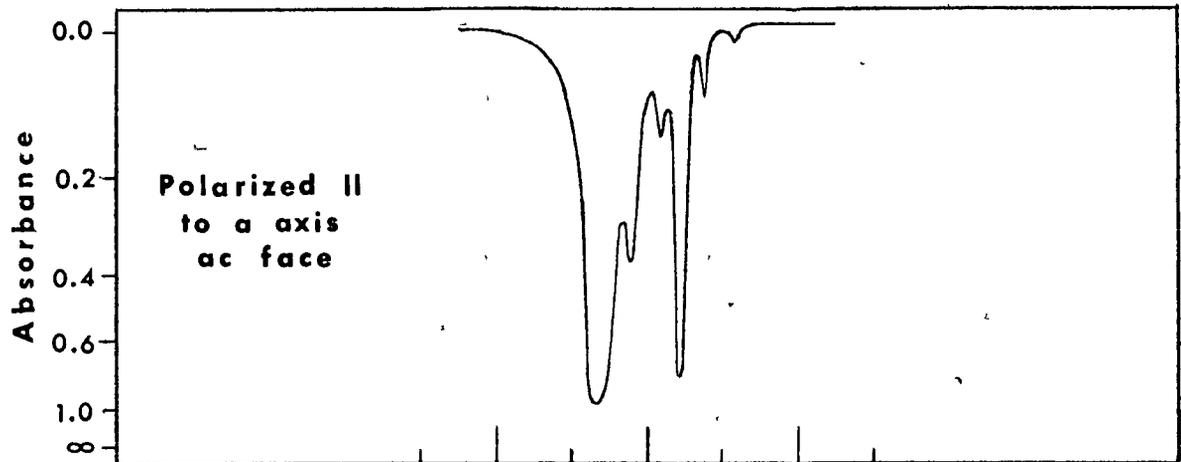
Frequency cm$^{-1}$

TABLE 3

VIBRATIONAL ASSIGNMENTS FOR SINGLE CRYSTAL

SPECTRA OF $Sr(CHO_2)_2$ (WAVENUMBERS IN $CM^{-1}$)

| Assignment* | X Active Modes | Y Active Modes | Z Active Modes |
|---|---|---|---|
| $\nu_3 - 15$ | 748 | | 748 |
| $\nu_3' - 23$ | 756 | | 756 |
| $\nu_3 - 12$ | 761 | | |
| $\nu_3$ | | | 763 |
| $\nu_3'$ | 766 | 766 | |
| $\nu_3 + 12$ | 775 | | 775 |
| $\nu_3'$ | | | 779.5 |
| $\nu_3'$ | 783.5 | | |
| $\nu_3 + 23$ | | 786 | 787 (sh) |
| $\nu_6$ | | 1067 | |
| $\nu_6$ | 1070 | | 1070 |
| $\nu_6'$ | 1084 | 1084 | |
| $\nu_6'$ | | | 1085 |
| $\nu_2$ | | 1360 | 1359 |
| $\nu_2'$ | 1363 | | |
| $\nu_2' + 10$ | | 1374 | |

TABLE 3 cont'd.

| Assignment* | X Active Modes | Y Active Modes | Z Active Modes |
|---|---|---|---|
| $\nu_5 - 10$ | | 1383 | |
| $\nu_5$ | 1393 | 1393 | |
| $\nu_5'$ | | 1399 | 1399 |
| $\nu_5 + 10$ | | 1403 | |
| $\nu_4 , \nu_4'$ | 1580 | 1580 | 1580 |
| $\nu_4 + 70$ | | | 1650 |
| $\nu_4 + 155$ | 1735 (sh) | 1735 (sh) | |
| $\nu_4 + 180$ | | | 1760 (sh) |
| $\nu_4 + 200$ | | | 1780 (sh) |
| $\nu_2 + \nu_3$ | | | 2130 |
| $\nu_2' + \nu_3'$ | 2152 | | |
| $\nu_3 + \nu_5$ | 2165 | 2165 | 2165 |
| $\nu_3 + \nu_4'$ | 2334 | 2334 | 2334 |
| $\nu_2 + \nu_6$ | 2434 | 2434 | 2434 |
| $\nu_2' + \nu_6'$ | | 2458 | 2458 |

TABLE 3 cont'd.

| Assignment* | X Active Modes | Y Active Modes | Z Active Modes |
|---|---|---|---|
| $2\nu_2$ | 2702 | 2702 | |
| $2\nu_2'$ | | 2721 | 2721 |
| $\nu_2 + \nu_5$ | 2735 | | |
| $\nu_2' + \nu_5'$ | 2753 | | |
| $2\nu_5$ | | 2760 | |
| $2\nu_5'$ | 2775 | | 2775 |
| $\nu_1 - 20$ | | 2852 | |
| $\nu_1, \nu_1'$ | 2872 | 2872 | 2872 |
| $\nu_2 + \nu_4$ | 2925 | 2925 | 2925 |
| | 2944 (sh) | 2944 (sh) | |
| $\nu_2' + \nu_4'$ | 2957 | 2957 (sh) | |
| $\nu_4 + \nu_5$ | | | 2975 |
| | | 2988 | |
| $\nu_4' + \nu_5'$ | 2998 (sh) | | 2998 (sh) |
| $2\nu_4$ | 3128 | | 3128 |
| | 3143 (sh) | | 3143 (sh) |
| $2\nu_4'$ | | | 3192 |
| $\nu_1 + \nu_3$ | 3631 | | 3631 |
| $\nu_1' + \nu_3'$ | 3648 | | |

* The $\nu$ and $\nu'$ refer respectively to formate ions I and II.

- 31 -

FIG 4-1 POLARIZED SPECTRA OF Sr(CHO$_2$)$_2$·2H$_2$O   3900-2500 cm$^{-1}$
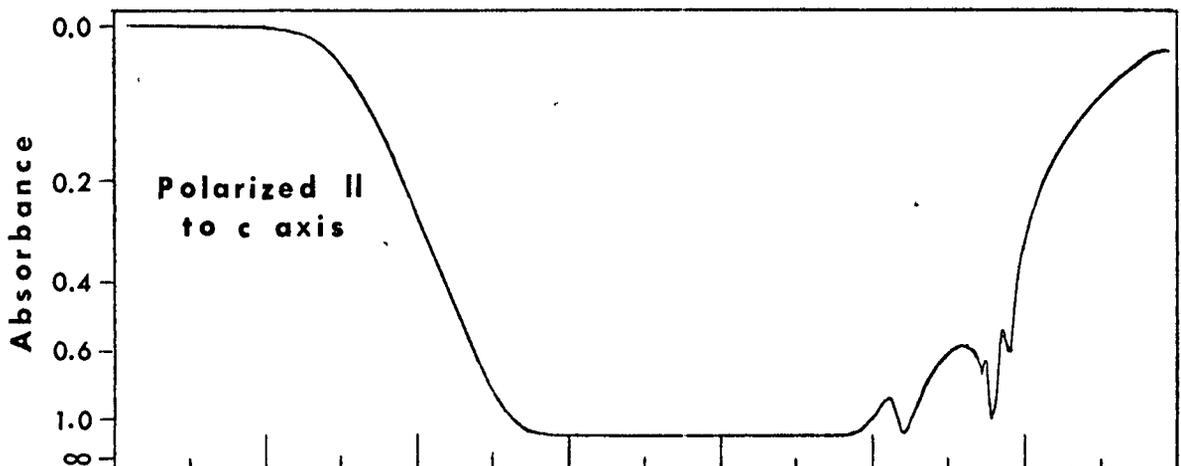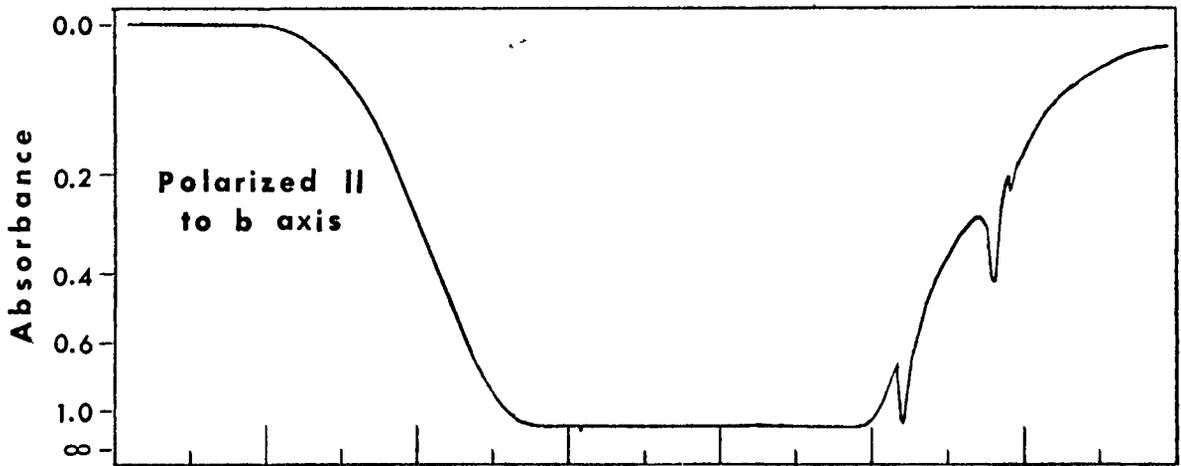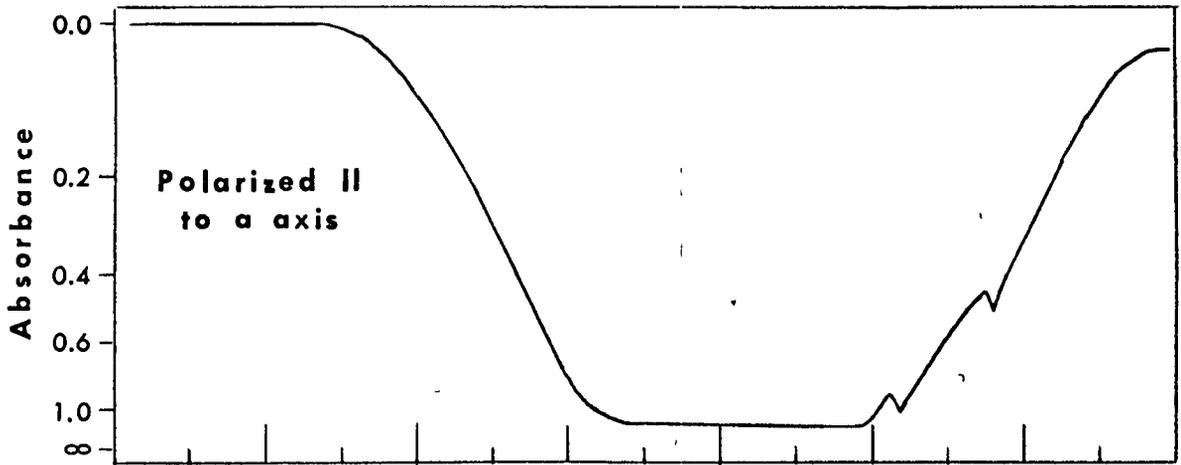
# FIG 4-2 POLARIZED SPECTRA OF $Sr(CHO_2)_2 \cdot 2H_2O$  2500-1900 cm$^{-1}$
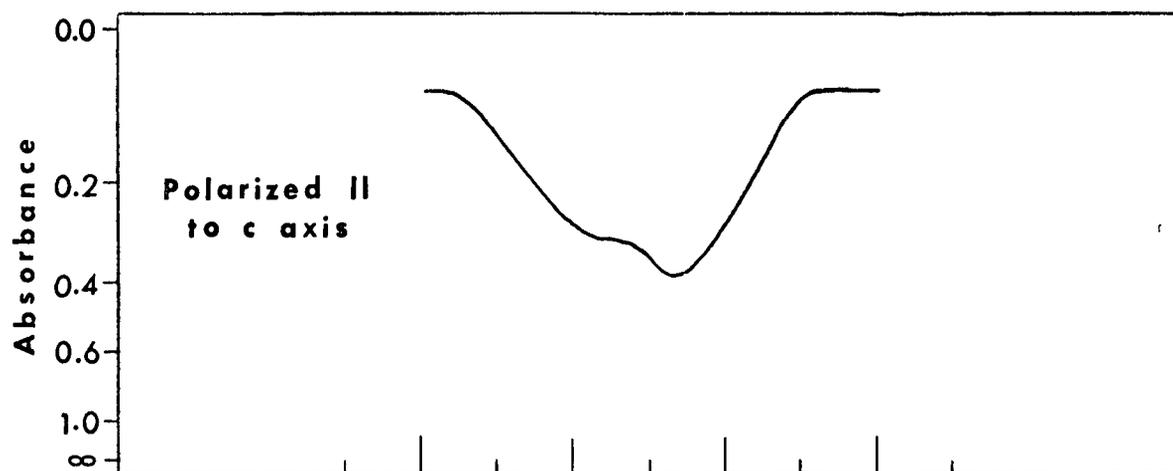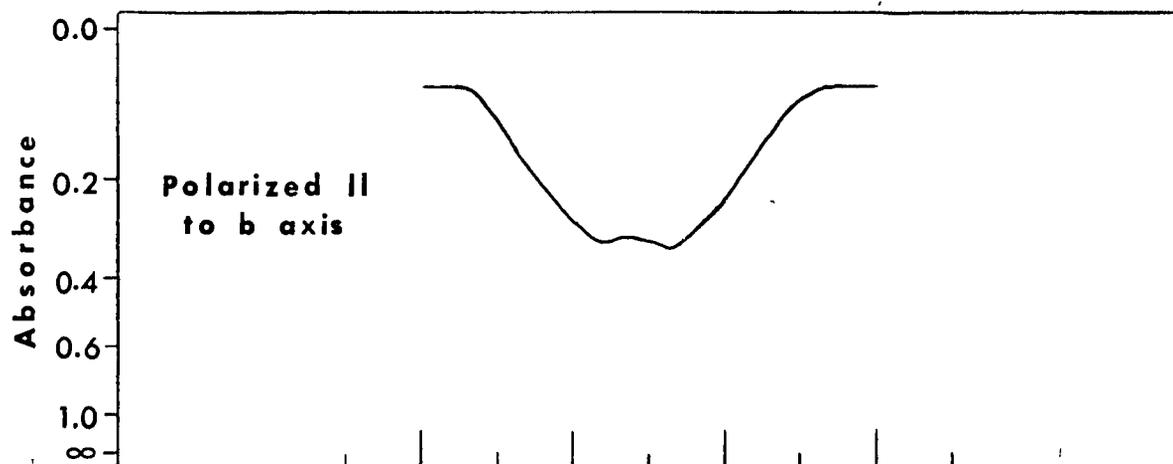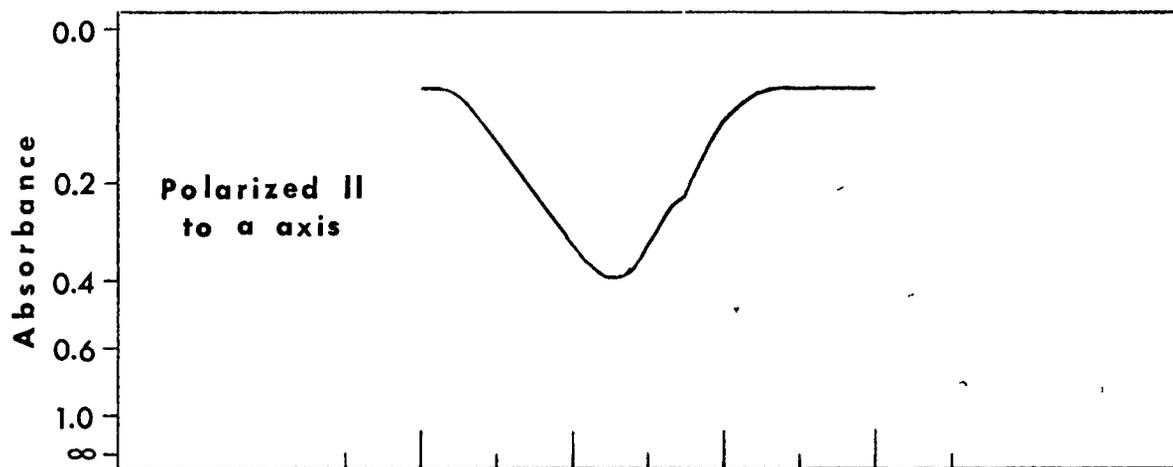
# FIG 4-3 POLARIZED SPECTRA OF Sr(CHO$_2$)$_2$·2H$_2$O   2000-1200 cm$^{-1}$
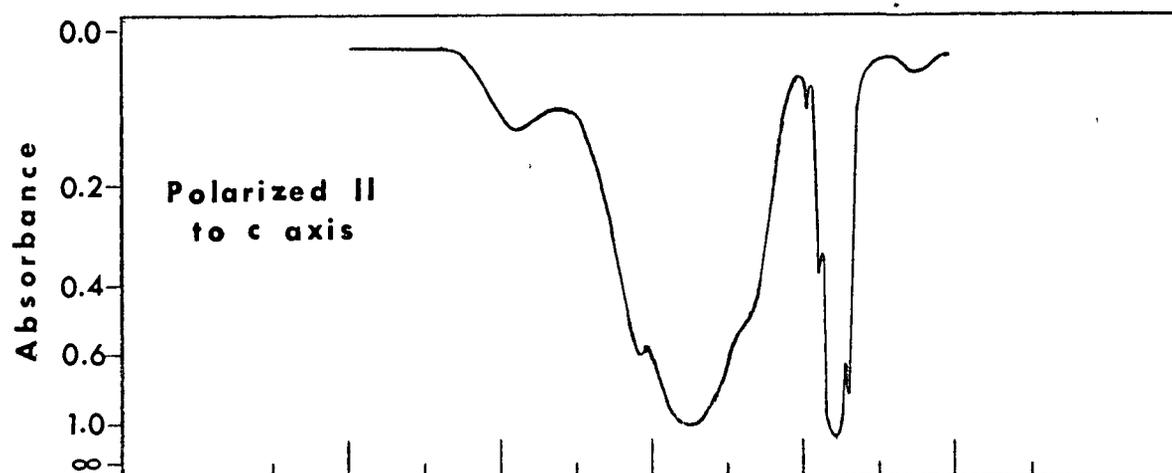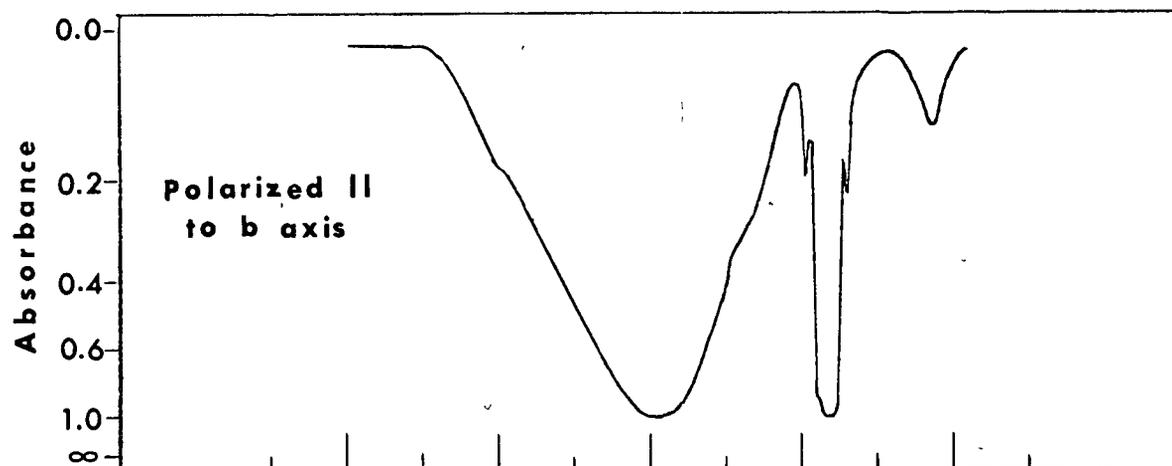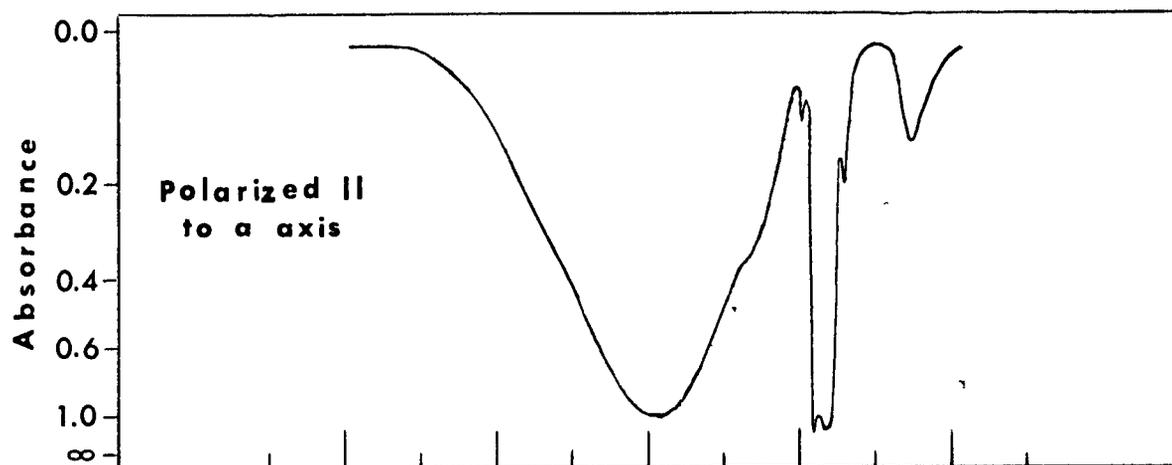
# FIG 4-4 POLARIZED SPECTRA OF Sr(CHO₂)₂·2H₂O   1100-500  cm⁻¹
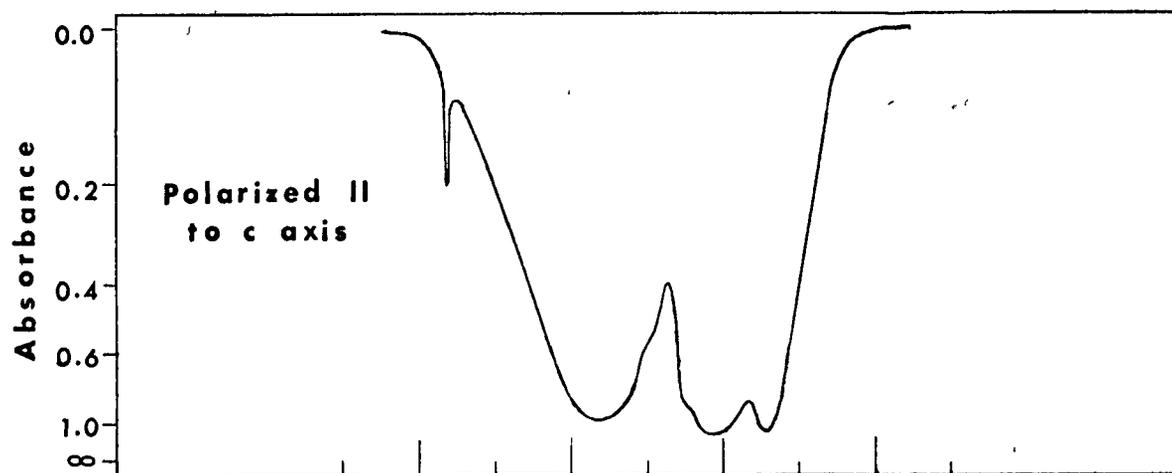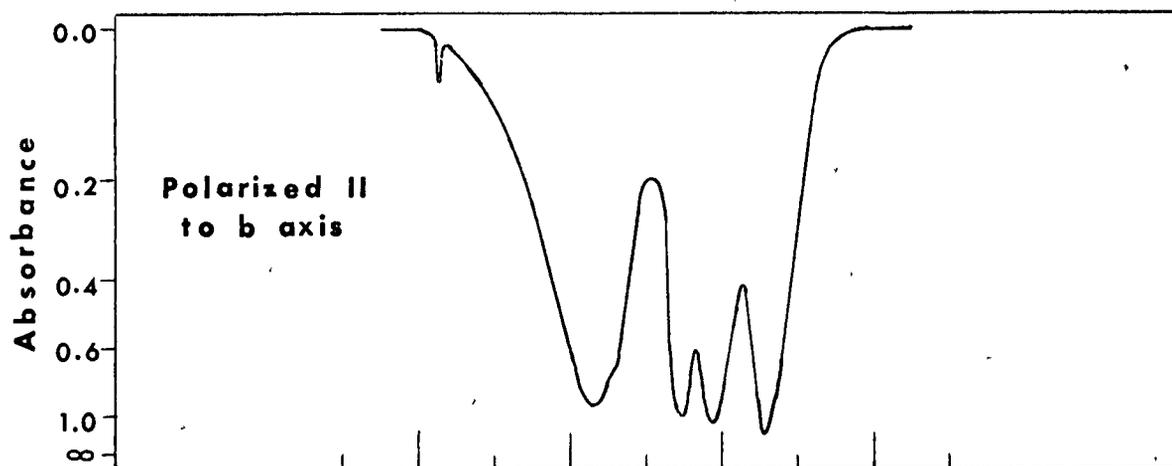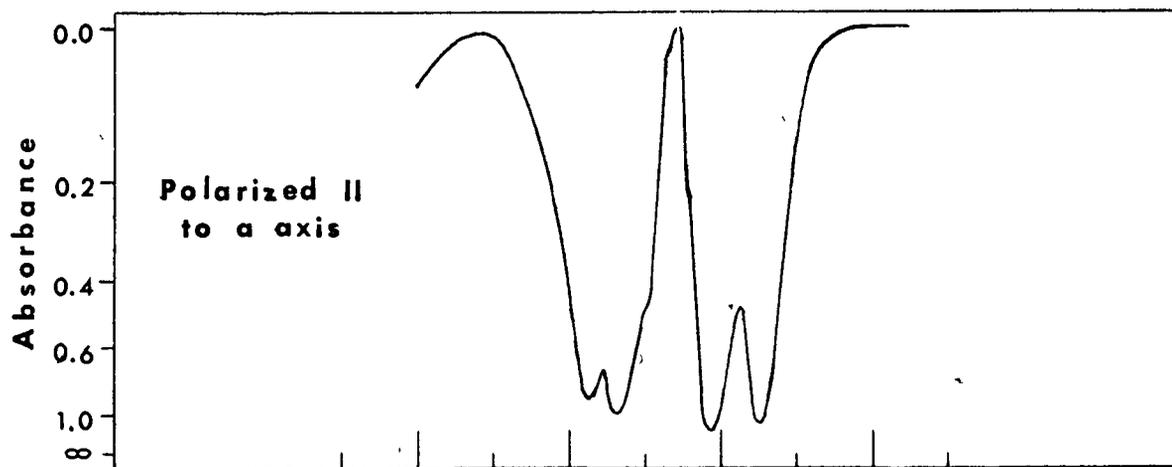
TABLE 4 - 1

## VIBRATIONAL ASSIGNMENTS FOR SINGLE CRYSTAL
## SPECTRA OF $Sr(CHO_2)_2 \cdot 2H_2O$ (WAVENUMBERS IN $CM^{-1}$)

| Assignment* | X Active Modes | Y Active Modes | Z Active Modes |
|---|---|---|---|
| $\nu_R(H_2O)_1$ | 642 | 642 | 642 |
| $\nu_R(H_2O)_2$ | 710 | 710 | 710 |
| $\nu_R(H_2O)_3$ | 750 (sh) | 750 | 753 (sh) |
| $\nu_R(H_2O)_4$ | 797 (sh) | | 797 (sh) |
| $\nu_R(H_2O)_5$ | 840 | 838 (sh) | |
| $\nu_R(H_2O)_6$ | | | 856 |
| $\nu_R(H_2O)_7$ | 872 | 872 | |
| $\nu_6 , \nu_6'$ | | 1064 | 1064 |
| | | 1225 | |
| $2\nu_R(H_2O)_1$ | 1255 | | 1255 |
| $\nu_2 - 18$ | 1337 | 1337 | 1337 |
| $\nu_2$ | | | 1355 |
| $\nu_2', \nu_5$ | 1364 | 1364 | |
| $\nu_5'$ | 1383 | 1383 (sh) | 1383 |
| $\nu_5 + 18$ | 1392 | 1392 | 1392 |

TABLE 4 - 1 cont'd.

| Assignment* | X<br>Active Modes | Y<br>Active Modes | Z<br>Active Modes |
|---|---|---|---|
| $\nu_4' - 110$ | 1476 (sh) | 1476 (sh) | 1476 (sh) |
| $\nu_2(H_2O)$ | | | 1545 |
| $\nu_4$ | 1590 | 1590 | |
| $\nu_4'$ | | | 1612 |
| $\nu_4' + 110$ | | 1700 (sh) | |
| $\nu_2(H_2O) + \nu_R(H_2O)_1$ | 2170 (sh) | 2170 | 2170 |
| $\nu_2(H_2O) + \nu_R(H_2O)_2$ | 2250 | 2250 | 2250 (sh) |
| $2\nu_2$ | | 2718 | 2718 |
| $2\nu_5$ | 2740 | 2740 | 2740 |
| $2\nu_5'$ | | | 2763 |
| $\nu_1 , \nu_1'$ | 2858 | 2858 | 2858 |
| $\nu_1(H_2O), \nu_3(H_2O)$ | 3150 | 3150 | 3150 |

* The $\nu$ and $\nu'$ refer respectively to formate ions I and II.

TABLE 4 - 2

VIBRATIONAL ASSIGNMENTS FOR SINGLE CRYSTAL

SPECTRA OF $Sr(CHO_2)_2 \cdot 2H_2O$ - PREVIOUS WORK*(WAVENUMBERS IN $CM^{-1}$)

| Assignment | X Active Modes | Y Active Modes | Z Active Modes |
|---|---|---|---|
| | 662 | 662 | 662 |
| $\nu_3$ | 714 | 714 | 714 |
| $\nu_3$ | | 757 | 757 |
| | | | 853 |
| | | 865 | |
| $\nu_2$ | 1370 | 1367 | 1366 |
| $\nu_4$ | 1377 | 1378 | |
| $\nu_4$ | 1387.5 | 1387.5 | |
| $\nu_5$ | 1614 | | |
| $\nu_5$ | | 1603 | |

* Vierne et al.

CHAPTER IV     THEORY

Sections 1 and 2 of this Chapter
briefly discuss the vibrations of a poly-
atomic system and the associated selection
rules, and are used as an aid in introducing
the more complex theory of solid state
spectra contained in sections 3 and 4.

4-1   The Vibrations of Isolated Polyatomic Molecules

In order to study the motions of an isolated n-atomic

system, a set of $3n$ coordinates is required to describe

its' configuration.  Of these $3n$ coordinates, three describe

the translational motion and three more describe the rotat-

ional motion of the system, leaving $3n-6$ coordinates to

describe the systems' vibrational degrees of freedom.

Wilson, Decius and Cross (13) discuss a general method

whereby the equations of motion may be written in terms of

a chosen coordinate system.  The set of equations thus

derived yields a series of solutions corresponding to the

normal modes of vibration of the system.

The $3n \times 3n$ secular determinant which must be solved in

order to determine the normal frequences can often be

simplified.  This simplification arises from the fact that

the system under investigation usually possesses some form

of symmetry.  If, in a molecule, a symmetry operation is

carried out which transforms the molecule into an equivalent
position, the kinetic and potential energies will remain
unchanged.

The set of symmetry operations that a molecule possesses
which carry it into equivalent positions is known as a
group. Each symmetry operation associated with the group
maybe represented analytically by a linear transformation
connecting the old coordinates with coordinates of the
molecule in its new position. The set of linear transform-
ations so obtained is said to be a representation of the
group of symmetry operations; while the coordinates, in
terms of which the transformation are written are said to
form a basis of the representation.

It is usually possible, by choosing a suitable set of
coordinates to reduce the $3n \times 3n$ transformation matrices
to a comparatively simple form; in effect separating these
coordinates into sets which do not mix with each other in
any of the transformations. When a coordinate system has
been found such that it is impossible to break the coordinates
down into any smaller non-mixing sets, the representation
for which these coordinates form a basis is said to be
completely reduced. When it is possible to do this, the
original representation is said to be reducible. The
equations involving the members of any one non-mixing set
can be considered by themselves as making up transformations

which form a representation of the group. Such a representation is irreducible and it is seen that a completely reduced representation is made up of a number of irreducible representations.

It is usually possible to choose several sets of coordinates to form a basis for the representations, but in each case the results would be the same. Any two representations,are said to be equivalent when they differ only in the choice of the basis coordinates.

The fundamental theorem concerning irreducible representations states that for each point group there are only a definite number of non-equivalent irreducible representations possible. It is possible to show that the number of times an irreducible representation appears in a reduced representation is

$$ n_i = \frac{1}{h} \sum_R \chi_R^i \chi_R \tag{1} $$

Where h is the order of the group (equal to the number of symmetry operations contained in the group), $\chi_R$ is the character of the reducible representation and $\chi_R^i$ is the character of the $i$th irreducible representation of the operation R . The sum is taken over all the operations of the group. The character is defined as the sum of the diagonal elements of the transformation matrix, the characters of equivalent representations being identical. These

quantities on the right hand side of (1) are easily deter-
mined using a simple set of rules.

Associated with each non-mixing set of normal coordinates
is a set of normal modes of vibration, the number of normal
modes being equal to the number of normal coordinates in the
set. Since each normal coordinate transforms according to
one of the irreducible representations of the group, we
can use (1) to determine the number of normal modes of
vibration belonging to each irreducible representation.


## 4-2 Selection Rules

Group theory maybe used to derive the selection rules
for vibrational transitions in the infrared. For a fund-
amental transition to occur by absorption of infrared
radiation it is necessary that one or more of the integrals:

$$\int \Psi_i^* \mu_x \Psi_j \, d\tau, \quad \int \Psi_i^* \mu_y \Psi_j \, d\tau, \quad \int \Psi_i^* \mu_z \Psi_j \, d\tau$$

have a non zero value. Here, $\Psi_i$ is the vibrational ground
state, $\Psi_j$ is the excited state and $\mu_x$, $\mu_y$, and $\mu_z$
are the components of the electric dipole moment operator.
It maybe determined whether the above integrals vanish if
the symmetry properties of $\Psi_i$, $\Psi_j$, $\mu_x$, $\mu_y$ and $\mu_z$
are known. Since these are definite integrals over the
whole configuration space of the molecule, they should be

unchanged by a symmetry operation R, in as much as such an operation merely produces a transformation of coordinates. That is, either the integrals must be totally symmetric, or the triple direct product of the species $\psi_\lambda$, $\mu$ and $\psi_j$ must contain the totally symmetric species.

Since all wave functions for normal vibrations in their ground states ( $\psi_i$ ) are bases for the totally symmetric representation of the symmetry species of the molecule, the integral for fundamental transitions (from the ground state to the first excited state) will be symmetric of the dipole moment operator and the first excited state belong to the same species (i.e. the direct product of a representation with itself is symmetric). It can be shown (10) that the components of the dipole moment operator transform in the same manner as the translational coordinates, $T_x$, $T_y$, and $T_z$. Thus a normal mode of vibration will be infrared active if $\psi_j$ belongs to the same symmetry species as one of the translational coordinates. Similar symmetry arguments may be applied to determine the activity of overtone and combination absorption. It should be noted that the above discussion considers dipole selection rules only- other interactions are assumed negligible.

## 4-3   Solid State Spectra and Crystal Symmetry

The discussion of the vibrations of polyatomic molecules
in 4-1 pertained to isolated molecules.  In crystals where
molecules are in close proximity to one another it is
necessary to consider the nature of the intermolecular
interactions when seeking to determine selection rules for
optical transitions.  Procedures for determining these
selection rules, have been devised by Bhagavantam and
Venkatarayudu (14) and also by Halford (15).  In the first
of these procedures the motions of the crystallographic
unit cell are considered whereas in that of Halford attention
is focused upon the motions of individual molecules.  It is
the work by Bhagavantam and Venkatarayudu that shall be
referred to most.  However, before proceeding it is
convenient to briefly consider the relation of various
groups to the description of crystal symmetry.

If a crystal were infinite in extent, it would admit
an infinite number of symmetry operations including trans-
lations, proper and improper rotations and combinations of
these.  There are a limited number of ways of combining
such operations to form the 230 space groups.  The symmetry
of a crystal maybe described by assigning it to the space
group which contains as its elements the symmetry operations
associated with the crystal.  It should be noted that crystals

on the basis of their external symmetry can be distributed
among 32 crystal classes, each class being identified with
a collection of symmetry elements and an unique point group
of operations concerned with them. Each point group
generates a characteristic number of space groups which,
as indicated above, are descriptive of the internal crystal
structure.

It is shown in standard works on space group theory
that any space group may be regarded as the product of an
invariant subgroup, known as a translation group, and a
factor group. The translation group as its name suggests
consists of the elements of the space group corresponding
to pure translations. As already indicated the cosets of
the translation group in the space group form what is known
as a factor group. The factor groups are always isomorphous
with one of the 32 crystallographic point groups, although
some of them may involve cosets containing other than
purely point operations combined with lattice translations
(i.e. screw rotation or glide reflection.)

The last group with which we will be concerned is the
site group. A site is defined as a point which is left
invariant by certain operations of the space group and is
equivalent to what is crystallographically known as a
special position. These operations may be shown to form a
group which is known as a site group. Every point in the

crystal lattice is thus a site, and is associated with at least the trivial site group $C_1$. A site group is necessarily isomorphous with some subgroup of the factor group and, of course, involves only point symmetry operations since no glide reflection or screw rotation can leave any point invariant.

The two procedures previously mentioned for determining selection rules associated with optical transitions in crystals, may now be more precisely described by stating the type of group used in the analysis of the motion; i.e. Bhagavantam and Venkatarayudu analyse the motion of the unit cell under the factor group and Halford analyses the molecular unit in the crystal according to the group associated with its site. In the following section the factor group analysis of Bhagavantam and Venkatarayudu which is generally more satisfactory than the site group analysis of Halford will be considered.

4-4   Factor Group Analysis of Vibrations in Crystals

As previously mentioned the factor group analysis considers the unit cell or more correctly the primitive unit cell of the crystal which by definition contains the smallest repeating unit of pattern found within the crystal (i.e. this unit of pattern is related to identical units of

pattern in all neighbouring unit cells by simple translation.)
For n atoms in the primitive unit cell there will be 3n
vibrations of which three correspond to vibrations associated
with translation of the unit cell. The remaining 3n-3
vibrational modes are classified as being either external
or internal vibrations. The external vibrations or lattice
vibrations are further classified as arising from trans-
latory or rotatory motions of the molecules in the unit cell.
The external vibrations usually exhibit low frequencies;
while the internal vibrations or vibrations involving
movements of the individual atoms in each molecule against
themselves will generally exhibit high frequencies.

By considering the group of n non-equivalent points,
corresponding to the n non-equivalent atoms contained in the
primitive unit cell and applying the principles of group
theory, we can find an expression for $n_i$ , the number of
times a particular irreducible representation $\Gamma j$ is
contained in the reducible representation $\Gamma$ . The derived
expression is:

$$n_i = \frac{1}{N} \sum_j h_j \chi_j(R) \chi(R) \qquad (2)$$

Where $\chi_j(R)$ and $\chi(R)$ are the characters of the operation
R in the representations $\Gamma_j$ and $\Gamma$ respectively; $N$ is
the order of the group and $h_j$ is the number of group
operations falling under the $j$th class. All terms in (2)

except $\chi(R)$ can be obtained from the appropriate factor group.  Analytical expressions for the $\chi(R)$ have been devised by Bhagavantam and Venkatarayudu (14) and are summarized in Table 5.

By suitable choice of the reducible representation and utilizing the characters $\chi(R)$ appropriate to it we can confine ourselves to one or the other of the several types of normal vibrations mentioned previously.  The type of normal vibration associated with each of the $\chi(R)$ is indicated in Table 5.

The factor group analysis for $Sr(CHO_2)_2$ and $Sr(CHO_2)_2 \cdot 2H_2O$ are given respectively in chapters V and VI.

SUMMARY OF EXPRESSIONS FOR CHARACTERS

OF THE GROUP OPERATIONS, R

| Type of Vibration | Expression for the Corresponding Characters of the Group Operation R in the Reducible Representation, $\Gamma$. |
|---|---|
| $n_i$ - Total number of vibrations of symmetry species i | $\chi(R) = U_R(n)(\pm 1 + 2\cos\phi)$ |
| $n_i(T)$ - Number of purely Translational vibrations of symmetry species i | $\chi(R) = (\pm 1 + 2\cos\phi)$ |
| $n_i(T')$ - Number of Lattice vibrations of Translational origin of symmetry species i | $\chi(R) = \left[U_R(s) - 1\right](\pm 1 + 2\cos\phi)$ |
| $n_i(R')$ - Number of Lattice vibrations of Rotational origin of symmetry species i | $\chi(R) = U_R(s-v)(1 \pm 2\cos\phi)$ |
| $n_i'$ - Number of Internal vibrations of symmetry species i | $\chi(R) = \left[U_R(n) - U_R(s)\right](\pm 1 + 2\cos\phi)$ $-U_R(s-v)(1 \pm 2\cos\phi)$ |

$U_R(n) =$ the number of atoms in variant under the operation R

$U_R(s) =$ the number of groups occupying lattice sites which are invariant under the operation R

$U_R(s-v) =$ the number of groups occupying lattice sites which are in variant under the operation R less the number of atoms occupying lattice sites which are invariant under the operation R

$\phi =$ the angle of rotation associated with the operation R.

CHAPTER V     DISCUSSION - PART I


This chapter discusses the experimentally observed infrared spectrum of crystalline $Sr(CHO_2)_2$ in relation to the vibrational modes predicted by the factor group analysis. In addition, information obtained from the polarized single crystal spectra is discussed in relation to the vibrational assignments and the crystal structure of $Sr(CHO_2)_2$. Lattice modes and combination modes are also discussed.


## 5-1  Vibrational Analysis for $Sr(CHO_2)_2$

As indicated in Chapter I the primitive unit cell of strontium formate contains 36 atoms; this means there will be a total of 108 vibrations. Using equation (2) we find that under the factor group $D_2^4$, which is isomorphous with the point group $D_2$, the structure of the representation of cartesian coordinates is $r = 27a + 27b_1 + 27b_2 + 27b_3$. By further application of equation (2) the types of normal vibrations associated with each irreducible representation can be determined. The results are summarized in the factor group analysis contained in Table 6.

Reference to Table 6 shows that there are a total of 48 internal vibrations: $12a , 12b_1 , 12b_2 , 12b_3$. This leaves 57 external vibrations which are distributed in the following manner; 36 lattice vibrations of rotatory origin:

TABLE 6

CHARACTER TABLE AND FACTOR-GROUP

ANALYSIS FOR $Sr(CHO2)_2$

| $D_2$ | E | $C_2(z)$ | $C_2(y)$ | $C_2(x)$ | $n_i$ | $n_i(T)$ | $n_i(T')$ | $n_i(R')$ | $n'_i$ | |
|---|---|---|---|---|---|---|---|---|---|---|
| a | 1 | 1 | 1 | 1 | 27 | 0 | 9 | 6 | 12 | |
| $b_1$ | 1 | 1 | -1 | -1 | 27 | 1 | 8 | 6 | 12 | $T_z$ |
| $b_2$ | 1 | -1 | 1 | -1 | 27 | 1 | 8 | 6 | 12 | $T_y$ |
| $b_3$ | 1 | -1 | -1 | 1 | 27 | 1 | 8 | 6 | 12 | $T_x$ |

$6a$ , $6b_1$ , $6b_2$ , $6b_3$ and 33 lattice vibrations of translatory origin: $9a$ , $8b_1$ , $8b_2$ , $8b_3$ . The remaining three vibrations correspond to translation on the unit cell and are of symmetry species $b_1$ , $b_2$ and $b_3$ .

## 5-2 The Internal Fundamentals of Sr(CHO$_2$)$_2$- Assignments

The significance of the splitting associated with the internal modes in relation to the free ion modes is understood by considering the relationship between the formate ions in the unit of pattern. For $Sr(CHO_2)_2$ the unit of pattern contains eight formate ions composed of two sets of four crystallographically equivalent units. In each set of four ions the ions may execute the same vibration in phase or $180°$ out of phase relative to one of their number arbitrarily chosen. Thus, for each set of four ions there are four possible combinations; each combinations corresponding to one of the irreducible representations of the $D_2^4$ factor-group and thus giving rise to crystal modes of $a$ , $b_1$ , $b_2$ and $b_3$ symmetry. It is readily seen that when this four-fold splitting associated with each set of four ions is considered with the two-fold splitting arising from the two sets of non-equivalent ions that we have an eight fold splitting associated with each of the six free ion fundamentals. Thus accounting for the 48 internal fundamentals

predicted by the factor-group analysis. However, since only species of $b_1$, $b_2$ and $b_3$ symmetry are active in the infrared the infrared spectrum of the crystal should reveal each fundamental associated with the free ion split into six components; giving rise to the 36 infrared active internal fundamentals.

It is readily seen from the factor group analysis that for polarized radiation along any one of the principal crystallographic axes only two of the six components are allowed; these two components corresponding to the two non-equivalent sets of formate ions contained in the unit of pattern.

Although the relative intensities of the internal fundaments are not discussed in detail until the next section; it is convenient to note that the intensity relation between the various components associated with the free ion fundamentals can be understood if we consider the direction cosines of the oscillating dipoles giving rise to the free ion fundamentals- to a first approximation the ratios of the relative intensities of the various components should be in the same ratio as the squares of the appropriate direction cosines.

Values for the squares of the direction cosines can be directly obtained from the crystal structure. The values given in Table 7 are based upon the crystal structure of

TABLE 7

## SQUARES OF THE DIRECTION COSINES

### FOR FORMATE IONS I AND II of $Sr(CHO_2)_2$

| Symmetry Species of Associated Free Ion Fundamentals | $l_1^2$ | $m_1^2$ | $n_1^2$ * |
|---|---|---|---|
| $a_1$ | 0.0659 | 0.0908 | 0.8431 |
| $b_1$ | 0.5320 | 0.4673 | 0.0007 |
| $b_2$ | 0.4039 | 0.4398 | 0.1563 |
|  | $l_2^2$ | $m_2^2$ | $n_2^2$ * |
| $a_1$ | 0.7510 | 0.0001 | 0.2490 |
| $b_1$ | 0.1777 | 0.2754 | 0.5469 |
| $b_2$ | 0.0711 | 0.7237 | 0.2053 |

\* The subscripts 1 and 2 refer to formate ions I and II respectively.

Nitta (9). In the following discussion it will be indicated where relative intensities have been used in making the assignments; reference being made to the spectra shown in Figures 2 and 3 and also to Tables 7 and 9 (Table 9- which is introduced later gives calculated and observed intensity ratios.)

The six free ion fundamentals of the formate ion have been well characterized (1-3), and as has been mentioned previously we expect each of the six free ion fundamentals to split into six infrared active components in the single crystal spectrum- thus giving rise to the 36 infrared active fundamentals predicted by the factor group analysis. It is convenient to discuss the internal fundamentals in terms of the free ion fundamentals. First of all we will consider the free ion fundamental $\nu_1(\nu CH)a_1$ as related to the crystal spectrum. Both the spectrum of polycrystalline $Sr(CHO_2)_2$ (Fig. 2-1) and the single crystal spectrum (Fig. 3-1) indicate only a single absorption corresponding to $\nu_1$; this absorption occurring at 2872 cm$^{-1}$. That no observable splitting occurs is further verified by the fact that the intensity ratios expected for various polarizations, assuming no splitting are in good agreement with the ratios observed experimentally (Table 9).

For $\nu_2(\nu CO)a_1$ the polycrystalline spectrum (Fig. 2-2) shows three components occurring at 1359.5, 1362.5 and

$1368$ cm$^{-1}$; the two high frequency components appearing as well defined shoulders. The polycrystalline spectrum also shows another absorption in this region at $1349.5$ cm$^{-1}$. However, consideration of the spectrum of polycrystalline strontium formate -$d_1$ (Fig. 2-2) and the intensities shown by the polarized single crystal spectra (Fig. 3-2) indicate that this absorption is not associated with $\nu_2$. Considering the $\nu_2$ region in the spectrum of polycrystalline strontium formate -$d_1$ we see that no corresponding absorption appears which immediately suggests that the absorption under consideration is not associated with $\nu_2$. It is also interesting to note that even though the spectrum of polycrystalline strontium formate -$d_1$ shows no evidence of splitting in the

region- the band envelope indicates that the same splitting is present as for polycrystalline strontium formate. Although the $\nu_2$ region is not very well resolved in the single crystal spectra, the use of polarized radiation shows that the $1359.5$ cm$^{-1}$ component is due to ion I while the components occurring at $1362.5$ cm$^{-1}$ and $1368$ cm$^{-1}$ are due to ion II. In the single crystal spectra, under X polarization the most intense absorption occurring in this region is found at $1362$ cm$^{-1}$ - reference to Table 7 shows that ion II is indicated. For Y polarization the most intense absorption occurs at $1359$ cm$^{-1}$ which indicates ion I. Under Z polarization we have the appearance of a broad absorption which

has a peak at 1360 cm$^{-1}$; this indicates the presence of the
1359.5 cm$^{-1}$ component associated with ion I, which we expect
to be strongly absorbing and also the presence of the
1368 cm$^{-1}$ component observed in the polycrystalline spectrum,
which we can assign to ion II.

The $\nu_3(\delta OCO)a_1$ region is well resolved in both the
polycrystalline and single crystal spectra (Figs. 2-3 and
3-4, 3-5 respectively). The polycrystalline spectrum shows
three well resolved absorptions occurring at 763, 779.5 and
783.5 cm$^{-1}$. The intensity ratio of the two high wave
number absorptions is approximately one-third. Reference to
Table 7 immediately indicates that ion II is involved; the
less strongly absorbing 779.5 cm$^{-1}$ absorption being the X
active component and the 783.5 cm$^{-1}$ absorption being the Z
active component. As shown in Table 9 the intensity ratios
obtained from the single crystal spectra support this
assignment. The remaining component of the triplet, occurr-
ing at 763 cm$^{-1}$ is thus due to ion I and reference to Table 7
indicates it should be most active under Z polarization.
Reference to the single crystal spectra show that under Z
polarization a doublet unexpectly appears in this region.
For the Z polarized bc face a peak occurs at 766 cm$^{-1}$ with
a shoulder occurring at 761 cm$^{-1}$; for the Z polarized ac
face the situation is reversed. It is possible that the
peaks occur because of the Y active 766 cm$^{-1}$ absorption and

the X active 761 cm$^{-1}$ absorption. Rationalizing in this manner enables us to place the Z active component at 763 cm$^{-1}$ as indicated by the polycrystalline spectrum. Consideration of intensity ratios show that the less strongly absorbing X and Y active components both occur at 766 cm$^{-1}$. As indicated in Table 9 the calculated and observed intensity ratios for this region are in excellent agreement. It is also interesting to note that identical splitting is observed in the $\nu_3$ region in the polycrystalline spectra of both Sr(CHO$_2$)$_2$ and Sr(CDO$_2$)$_2$.

The most intense region of absorption observed in the spectrum of crystalline strontium formate is associated with the free ion fundamental $\nu_4(\nu CO)b_1$ . This region is best resolved in the polycrystalline spectra; in the spectrum of both polycrystalline strontium formate and polycrystalline strontium formate d$_1$ (Fig. 2-1) almost identical splitting into a doublet is observed. In the spectrum of polycrystalline strontium formate the components of the doublet are observed at 1570 and 1593 cm$^{-1}$. The single crystal spectra for all three polarizations (Fig. 3-2) show only a strong absorption at about 1580 cm$^{-1}$; as expected the intensity of this absorption is least under Z polarization. It was not possible to assign either member of the doublet to ion I or II on the basis of the polarized spectra. However, it has been seen that for both $\nu_2$ and $\nu_3$ the high wave number member of the

doublet has been associated with ion I and as will be seen this order is preserved for the $_5$ and $_6$, and on this basis we can tentatively assign the 1570 cm$^{-1}$ component to ion I and the 1593 cm$^{-1}$ component to ion II.

Reference to the spectrum of polycrystalline strontium formate (Fig. 2-2) shows a well resolved doublet associated with the free ion fundamental $\nu_5 (\omega CH) b_1$; the components of this doublet occur at 1393.5 and 1399 cm$^{-1}$. Although the single crystal spectra (Fig. 3-2) are not very well resolved in this region it can be seen that for X polarization a strong absorption at 1393 cm$^{-1}$ appears. Reference to Table 7 shows this indicates ion I. Under Y polarization there is a strong absorption occurring at 1396 cm$^{-1}$ which appears to be split into a doublet indicating the appearance of both components. For Z polarization a sharp peak at 1399 cm$^{-1}$ appears indicating ion II as expected.

Finally we consider the free ion fundamental $\nu_6 (\rho CH) b_2$. This mode is observed only with difficulty in the spectrum of polycrystalline $Sr(CHO_2)_2$ (Fig. 2-1). When it is observed it appears as a very weak absorption occurring at 1084 cm$^{-1}$. The single crystal spectra (Fig. 3-3) show a doublet in this region. Under X polarization the members of the doublet occur at 1070 and 1084 cm$^{-1}$, under Y polarization at 1067 and 1084 cm$^{-1}$ and under Z polarization at 1085 and 1070 cm$^{-1}$. As shown in the spectra there are marked

differences in intensity for the various components and
reference to Table 7 allows us to assign the high wave
number component to ion II and the low wave number component
to ion I.

Table 8 gives a complete summary of the results discussed
above. From the table we can see the magnitude of the
various splittings. The splitting associated with the doublet
is a direct measure of the static field effect while the
splitting associated with the triplets is a direct measure
of the dynamic crystal effect or correlation field splitting.

### 5-3   The Internal Fundamentals of $Sr(CHO_2)_2$- Intensities

The relation of the intensity of the internal fund-
amentals to the direction cosines of the oscillating dipoles
giving rise to the free-ion fundamentals was mentioned in
the previous section. In this section observed intensity
ratios are presented along with the corresponding calculated
ratios. For each of $\nu_3$ and $\nu_6$ two sets of ratios corres-
ponding to the intensities arising from formate ions I and
II were obtained. While for each of $\nu_1$, $\nu_2$, $\nu_4$ and $\nu_5$
it was only possible to obtain a single set of intensity
ratios; the ratios corresponding to the combined intensities
arising from formate ions I and II. The results are
contained in Table 9 and especially for the well resolved

TABLE 8

## THE INTERNAL FUNDAMENTAL MODES

## OF $Sr(CHO_2)_2$ (WAVENUMBERS IN $CM^{-1}$)

| Free Ion Fundamental* | Associated Doublet† | Magnitude of Splitting | X Active $b_3$ Modes | Y Active $b_2$ Modes | Z Active $b_1$ Modes† |
|---|---|---|---|---|---|
| $\nu_1(\nu CH)a_1$ | 2872 | 0 | ? | 2872 | 2872 |
| $\nu_1'$ | 2872 | | 2872 | — | ? |
| $\nu_2(\nu CO)a_1$ | 1359.5 | | ? | ? | 1359 |
| $\nu_2'$ | 1365 | 5.5 | 1363 | — | 1368 |
| $\nu_3(\delta OCO)a_1$ | 763 | | 766 | 766 | 763 |
| $\nu_3'$ | 781.5 | 5.5 | 783.5 | | 779.5 |
| $\nu_4(\nu CO)b_2$ | 1570 | | ? | ? | — |
| $\nu_4'$ | 1593 | 23 | ? | ? | ? |
| $\nu_5(\omega CH)b_1$ | 1393.5 | | 1393 | 1393 | — |
| $\nu_5'$ | 1399 | 5.5 | ? | ? | 1399 |
| $\nu_6(\rho CH)b_2$ | 1084 | | 1084 | 1084 | 1085 |
| $\nu_6'$ | 1069 | 15 | 1070 | 1067 | 1070 |

* The $\nu$ and $\nu'$ refer to formate ions I and II respectively.

† The frequencies for the components of the doublet are given as averages of the X, Y and Z active components where necessary.

‡ The dashes (—) indicate that the corresponding activity is too weak to be observed experimentally, while the question marks (?) indicate that no conclusive assignments could be made from the observed spectra.

TABLE 9

**CALCULATED AND OBSERVED INTENSITY RATIOS — $Sr(CHO_2)_2$**

| Associated Free Ion Fundamental | $l_1^2/m_1^2$ | | | $m_1^2/n_1^2$ | | | $n_1^2/l_1^2$ | | | Product of Obs. Ratios |
|---|---|---|---|---|---|---|---|---|---|---|
| | Calc. | Obs. | % Error | Calc. | Obs. | % Error | Calc. | Obs. | % Error | |
| $\nu_3(a_1)$ | 0.726 | 0.712 | 1.9% | 0.108 | 0.107 | 0.9% | 12.8 | 12.4 | 3.1% | 0.945 |
| $\nu_6(b_2)$ | 0.918 | 1.000 | 8.9% | 2.81 | 2.67 | 5.0% | 0.387 | 0.375 | 3.1% | 1.001 |

| | $l_2^2/m_2^2$ | | | $m_2^2/n_2^2$ | | | $n_2^2/l_2^2$ | | | |
|---|---|---|---|---|---|---|---|---|---|---|
| | Calc. | Obs. | | Calc. | Obs. | | Calc. | Obs. | | |
| $\nu_3(a_1)$ | 7500 | | | 0.0004 | | | 0.332 | 0.375 | 13% | |
| $\nu_6(b_2)$ | 0.0982 | 0.0845 | 14% | 3.53 | 3.85 | 9.1% | 2.89 | 2.72 | 5.9% | 0.885 |

| | $l_1^2+l_2^2/m_1^2+m_2^2$ | | | $m_1^2+m_2^2/n_1^2+n_2^2$ | | | $n_1^2+n_2^2/l_1^2+l_2^2$ | | | |
|---|---|---|---|---|---|---|---|---|---|---|
| | Calc. | Obs. | | Calc. | Obs. | | Calc. | Obs. | | |
| $\nu_1(a_1)$ | 8.99 | 9.22 | 2.6% | 0.0832 | 0.0833 | 0.0% | 1.34 | 1.30 | 3.0% | 0.998 |
| $\nu_2(a_1)$ | 8.99 | 2.20 | 75% | 0.0832 | 0.314 | 280% | 1.34 | 1.25 | 6.7% | 0.864 |
| $\nu_4(b_1)$ | 0.956 | 1.12 | 17% | 1.36 | 1.51 | 11% | 0.772 | 0.597 | 23% | 1.010 |
| $\nu_5(b_1)$ | 0.956 | 1.35 | 41% | 1.36 | 1.30 | 4.4% | 0.772 | 0.592 | 23% | 1.040 |

regions of the spectrum, there is remarkably good agreement
between the experimental and calculated ratios. Since
each ratio was obtained from the polarized spectra of a
single sample no error is introduced into the ratios by
having to allow for sample thickness.

However, possible errors do arise from the following
sources:

(i)  the crystal slices were not ground absolutely
perpendicular to the crystal axes- the maximum deviation
being estimated at $2^{o}$ by observation of interference figures.

(ii)  the polarizer was not 100% efficient- it was
estimated that less than 5% of the component perpendicular
to the desired component was passed; measurements being made
in the visible region against a Wollaston prism.

(iii)  the incident radiation was not parallel due to
convergence of the sample beam- measurements of the con-
vergence showed that less than 1% of the component parallel
to the beam would be introduced.

(iv)  the polarizer was not correctly aligned with
respect to the sample face- it was estimated that the error
in alignment was less than $2^{o}$.

Consideration of the above sources of error suggest
that the experimental error introduced into the observed
intensity ratios could correspond to as much as 8% of the
component perpendicular to the desired component being passed.

However, it would appear from this study that if careful experimental procedure is followed the total error should correspond to less than 5% of the component perpendicular to the desired component being passed. Even so, it can be readily appreciated that if a certain component is strongly absorbing at a certain frequency under one polarization and is only very weakly absorbing at the same frequency under a different polarization; considerable error could be introduced into the observed intensity ratio.

In Table 9 the % error for each ratio is given as well as the product of the three ratios making up each set of ratios. This product should equal unity and the deviation from unity is a measure of the internal consistency possessed by the experimental intensities. Since the $\nu_2$, $\nu_4$ and $\nu_5$ regions are not very well resolved in the single crystal spectra we expect the greater error associated with the observed intensity ratios- the error being largely introduced by overlapping with combination modes.

One of the most interesting aspects of an infrared study of the crystalline state is the possibility of experimentally obtaining the direction cosines associated with the absorbing species. Reference to Table 9 shows that the intensity data for $\nu_1(a_1)$, $\nu_3(a_1)$ and $\nu_6(b_2)$ should allow direct calculation of the direction cosines associated with symmetry species $a_1$ and $b_2$ for both formate ions I and II. The only

problem which presents itself is that in some cases the product of the set of ratios is not internally consistent (i.e. the product does not equal unity). If this product is not equal to unity it can be readily appreciated that the direction cosines we calculate from the ratios will not be internally consistent themselves (i.e. the sum of their squares will not equal unity). In order to circumvent this problem each ratio in a set was multiplied by a common factor so as to bring the product of the ratios to unity. It is noted that this procedure is not justifiable mathematically but since this common factor in all cases was close to unity the error introduced is very small.

The signs of the direction cosines associated with the symmetry species $a_1$ and $b_2$ for both formate ions are obtained by applying the orthogonality requirement. Further application of the orthogonality relation allows calculation for both ions I and II of the direction cosines associated with symmetry species $b_1$.

The calculated and experimental direction cosines are contained in Table 10 and it can be seen that the agreement is exceptionally good.

TABLE 10

CALCULATED AND EXPERIMENTAL DIRECTION COSINES FOR FORMATE IONS I AND II OF $Sr(CHO_2)_2$

| Symmetry Species of Associated Free Ion Fundamentals | $l_1$ | | $m_1$ | | $n_1$ | |
|---|---|---|---|---|---|---|
| | Calc. | Expt'l | Calc. | Expt'l | Calc. | Expt'l |
| $a_1$ | -0.257 | -0.259 | 0.301 | 0.297 | 0.918 | 0.916 |
| $b_1$ | 0.729 | 0.715 | 0.684 | 0.699 | -0.026 | -0.025 |
| $b_2$ | 0.636 | 0.649 | -0.663 | -0.649 | 0.395 | 0.397 |

| | $l_2$ | | $m_2$ | | $n_2$ | |
|---|---|---|---|---|---|---|
| | Calc. | Expt'l | Calc. | Expt'l | Calc. | Expt'l |
| $a_1$ | -0.867 | -0.874 | 0.008 | 0.045 | -0.499 | -0.492 |
| $b_1$ | -0.421 | -0.405 | 0.525 | 0.501 | 0.740 | 0.765 |
| $b_2$ | -0.267 | -0.256 | -0.851 | -0.864 | 0.453 | 0.431 |

## 5-4 Overtones and Combinations of Internal Fundamentals-Sr(CHO$_2$)$_2$

As noted previously each free-ion fundamental is split into 8 components under the D$_2$ factor group. Of these 8 components 4 are associated with formate ions I and 4 are associated with formate ions II. Reference to Table 11 shows that the overtones associated with the internal fundamentals arising from formate ion I and also formate ion II consist of 16 components (4a , 4b$_1$, 4b$_2$, 4b$_3$). Of these 16 components 12 are infrared active (4b$_1$, 4b$_2$, 4b$_3$). Hence, we expect to observe 4 components for both ions I and II under each of X, Y and Z polarizations. Considerations similar to the above also apply to combination modes.

From the observed spectra it was possible to assign a number of overtones and combinations of internal fundamentals. These assignments were given previously in Table 3.


## 5-5 Combinations of Internal Fundamentals and Lattice Modes-Sr(CHO$_2$)$_2$

Sum and difference modes of the low frequency lattice vibrations and the internal fundamentals will give rise to a series of weaker peaks on the high and low frequency sides of the absorption peak assigned to the internal fundamental. The transition probabilities for the difference modes are the same as those of the corresponding sum modes but the

intensities are expected to be less because of the smaller populations of the excited lattice mode energy levels at which the transitions originate.

Reference to Table 6 shows that the lattice vibrations are distributed in the following manner: ($15a_1$, $14b_1$, $14b_2$, $14b_3$). If we consider the possible combinations of these lattice modes with the internal fundamentals we find by refering to Table 11 that for internal fundamentals of symmetry species, a, $b_1$, $b_2$ and $b_3$ the respective combination modes possible are: ($15a$, $14b_1$, $14b_2$, $14b_3$), ($15b_1$, $14a$, $14b_3$, $14b_2$), ($15b_2$, $14b_3$, $14a$, $14b_1$) and ($15b_3$, $14b_2$, $14b_1$, $14a$).

Remembering that crystal modes of symmetry species a are not infrared active it can be readily seen from the above that for each of X, Y and Z polarized spectra we would, in principle, expect the satellite structure of each of the 6 internal fundamental doublets to exhibit 114 peaks. Of these 114 peaks 57 will correspond to combination modes and the remaining 57 will correspond to difference modes.

From the observed spectra it was possible to tentatively assign a few lattice modes (Table 3). These assignments are based on the recurrence of identical peak separations between the various internal fundamentals and the modes associated with their satellite structures.

Reference to Table 3 shows that the observed spectrum indicates lattice modes occurring at 10, 12, 15, 20, 23, 70, 155, 180 and 200 cm$^{-1}$.

TABLE 11

SYMMETRY SPECIES OF

COMBINATIONS AND OVERTONES

| | a | $b_1$ | $b_2$ | $b_3$ |
|---|---|---|---|---|
| a | a | $b_1$ | $b_2$ | $b_3$ |
| $b_1$ | $b_1$ | a | $b_3$ | $b_2$ |
| $b_2$ | $b_2$ | $b_3$ | a | $b_1$ |
| $b_3$ | $b_3$ | $b_2$ | $b_1$ | a |

CHAPTER VI    DISCUSSION - PART II

This chapter discusses the experimentally observed infrared spectrum of crystalline $Sr(CHO_2)_2 \cdot 2H_2O$ in relation to the vibrational modes predicted by the factor group analysis. In addition information obtained from the polarized single crystal spectra is discussed, where possible in relation to the vibrational assignments and crystal structure of $Sr(CHO_2)_2 \cdot 2H_2O$. Lattice modes and combination modes are also discussed.

6-1   Vibrational Analysis for $Sr(CHO_2)_2 \cdot 2H_2O$

The vibrational analysis for $Sr(CHO_2)_2 \cdot 2H_2O$ is

contained in Table 12.   Since the space group for $Sr(CHO_2)_2 \cdot$

$2H_2O$ and $Sr(CHO_2)_2$ are both $P2_12_12_1$ $(D_2^4)$ little can be

added to the discussion contained in section 5-1.   We do

note however that for each of the 18 internal fundamental

vibrations associated with each symmetry species, the 12

modes- $n_i'(CHO_2)$ will be due to the formate ions and the

remain six modes- $n_i'(H_2O)$ will be due to the water molecules.

The internal fundamentals associated with the two non

equivalent water molecules contained in the unit of pattern

can be discussed in a manner entirely equivalent to the

discussion of the two non equivalent formate ions.

TABLE 12

CHARACTER TABLE AND FACTOR-GROUP

ANALYSIS FOR $Sr(CHO_2)_2 \cdot 2H_2O$

| $D_2$ | E | $C_2(z)$ | $C_2(y)$ | $C_2(x)$ | $n_i$ | $n_i(T)$ | $n_i(T')$ | $n_i(R')$ | $n_i'$ | $n_i'(CHO_2)$ | $n_i'(H_2O)$ | |
|---|---|---|---|---|---|---|---|---|---|---|---|---|
| $a$ | 1 | 1 | 1 | 1 | 45 | 0 | 15 | 12 | 18 | 12 | 6 | |
| $b_1$ | 1 | 1 | -1 | -1 | 45 | 1 | 14 | 12 | 18 | 12 | 6 | $T_z$ |
| $b_2$ | 1 | -1 | 1 | -1 | 45 | 1 | 14 | 12 | 18 | 12 | 6 | $T_y$ |
| $b_3$ | 1 | -1 | -1 | 1 | 45 | 1 | 14 | 12 | 18 | 12 | 6 | $T_x$ |

## 6-2   The Internal Fundamentals of $Sr(CHO_2)_2.2H_2O$- Assignments

The method of assignment used for the formate ions of $Sr(CHO_2)_2$ will also be used in the assignment of the internal fundamentals of $Sr(CHO_2)_2.2H_2O$.   The internal fundamentals associated with the formate ion as the absorbing species are considered first.

Reference to the single crystal spectra contained in Fig. 4-1 shows that in the region 3400-2900 $cm^{-1}$ there is unfortunately total absorption due to the O-H stretching frequencies of the water molecules.  However, this region of total absorption is not so broad so as to totally obscure the appearance of the internal fundamentals associated with $\nu_1$($\nu$CH)$a_1$ which appears at 2858 $cm^{-1}$ .  As for $Sr(CHO_2)_2$ there appears to be no observable splitting under various polarizations.

In the 1400-1300 $cm^{-1}$ region of the spectrum (Fig.4-3) there appears to be considerable overlapping of the various modes.  However, consideration of the relative intensities predicted by the squared direction cosines (Table 13) along with the information obtained from the polarized spectra allow us to make some fairly conclusive assignments.  Under X polarization we find the appearance of two strong absorptions occurring at 1383 and 1364 $cm^{-1}$.  Assuming that the order of the modes associated with the free-ion fundamentals

TABLE 13

SQUARES OF THE DIRECTION COSINES

FOR FORMATE IONS I AND II of $Sr(CHO_2)_2 \cdot 2H_2O$

| Symmetry Species of Associated Free Ion Fundamentls | $l_1^2$ | $m_1^2$ | $n_1^2$ * |
|---|---|---|---|
| $a_1$ | 0.0053 | 0.0011 | 0.9936 |
| $b_1$ | 0.3518 | 0.6482 | 0.0001 |
| $b_2$ | 0.6435 | 0.3505 | 0.0061 |
| | $l_2^2$ | $m_2^2$ | $n_2^2$ * |
| $a_1$ | 0.1599 | 0.8339 | 0.0063 |
| $b_1$ | 0.7987 | 0.1376 | 0.0638 |
| $b_2$ | 0.0405 | 0.0294 | 0.9301 |

\* The subscripts 1 and 2 refer to formate ions I and II respectively.

$\nu_2$ and $\nu_5$ is not reversed- reference to Table 13 indicates that the absorption occurring at 1383 cm$^{-1}$ is associated with the free ion fundamental $\nu_5(\omega\text{CH})b_1$ - ion II. The absorption occurring at 1364 cm$^{-1}$ also appears under Y polarization along with a shoulder at 1383 cm$^{-1}$, - it would appear that the 1364 cm$^{-1}$ absorption is due to a mixing of absorptions arising from $\nu_3$- ion I and $\nu_2$- ion II. Under Z polarization a strong absorption appears at 1355 cm$^{-1}$ - reference to Table 13 clearly indicates $\nu_2(\nu\text{CO})a_1$- ion II. As might be expected the absorption at 1383 cm$^{-1}$ due to $\nu_5$- ion II also appears under Z polarization. The two remaining absorptions appearing in this region at 1392 and 1337 cm$^{-1}$ appear to be due to combination modes.

The spectra contained in Fig. 4-4 show the appearance of $\nu_6(\rho\text{CH})b_2$ at 1064 cm$^{-1}$ - no splitting is observed. Unexpectedly no activity was observed for this mode under X polarization. However, for both Y and Z polarization where activity is observed it is noted the base line slopes "up" relative to the absorption in question while for X polarization the base line slopes "down". This difference in baseline position may account for the observed results. The spectra contained in Fig. 4-4 also show the region of the spectrum where we would expect to find the appearance of the modes associated with the free ion mode $\nu_3(\delta\text{OCO})a_1$. However, it is found that the strongly absorbing lattice

modes observed in this region totally obscure the appearance
of the internal fundamentals associated with $\nu_3(\delta OCO)a_1$.

The region of the spectrum associated with the free
ion fundamental $\nu_4(\nu CO)b_1$ (Fig. 4-3) like the other regions
where internal fundamentals are observed is complicated by
considerable overlapping. Under both X and Y polarizations
a very intense absorption occurs at 1590 cm$^{-1}$. However,
under Z polarization we find that we now have an intense
absorption occurring at 1545 cm$^{-1}$. Reference to Table 13
shows that we expect little intensity to be associated with

$_4$ under Z polarization. Hence, the above intensity
consideration when considered with the rather large shift
of 45 cm$^{-1}$ indicates the 1545 cm$^{-1}$ absorption as being
largely due to $\nu_2(\delta HOH)a_1$- the water molecules being the
absorbing species. Intensity ratios for this region-
considering the strong absorptions at 1590 and 1545 cm$^{-1}$ are
given in Table 15. If we consider the three strong absorp-
tions observed for the respective polarizations as being
due only to $\nu_4(CHO_2)$ and $\nu_2(H_2O)$ we can, in principle,
use the experimental intensity ratios to calculate values
for the sums of the squared direction cosines (i.e. $l_1^2 + l_2^2$
$m_1^2 + m_2^2$ and $n_1^2 + n_2^2$) associated with symmetry species
$a_1$ for water molecules I and II. However, when these sums
were calculated they were not consistent with the require-
ment that their total sum should equal two. This, of course,

indicates that other components are involved. None the less it can be said with a good deal of certainty that the observed intensity ratios show $\nu_2(H_2O)$ to be most strongly active under Z polarization and indicate strong Y activity.

Finally we consider the region of absorption associated with the O-H sketching frequencies. In discussing this region we can only consider the "dimensions" of the regions of total absorption. They are given below:

(i)   X polarization- 2875, 3100 and 3325 cm$^{-1}$

(ii)   Y polarization- 2925, 3175 and 3425 cm$^{-1}$

(iii) Z polarization- 2875, 3150 and 3425 cm$^{-1}$

In each of (i), (ii) and (iii) above the center wave number refers to the centre of the region of total absorption, with the two outside wave numbers referring to the outer extremities of the respective regions of total absorption. If we assume $\nu_2(H_2O)$ to be most strongly active under Y and Z polarizations, then consideration of the outer extremities of the regions of total absorption tends to place

$\nu_1(\nu OH)a_1$ - $H_2O$ at a higher frequency than $\nu_3(\nu OH)b_1$- $H_2O$.

The results discussed above are completely summarized in Table 14.

## 6-3   The Internal Fundamentals of Sr(CHO$_2$)$_2$.2H$_2$O- Intensities

Even though the polarized single crystal spectra of Sr(CHO$_2$)$_2$.2H$_2$O offer little intensity information of a

TABLE 14

## THE INTERNAL FUNDAMENTAL MODES

## OF $Sr(CHO_2)_2 \cdot 2H_2O$ (WAVENUMBERS IN $CM^{-1}$)

(i)  The Internal Fundamentals - $n_i{}'(CHO_2)_2$

| Free Ion *<br>Fundamental | $n_i{}'(CHO_2)$ | Observed<br>Activity |
|---|---|---|
| $\nu_1(\nu CH)a_1$ | 2858 | |
| $\nu_1{}'$ | 2858 | X, Y, Z |
| $\nu_2(\nu CO)a_1$ | 1355 | Z |
| $\nu_2{}'$ | ~1364 | X, Y |
| $\nu_3(\delta OCO)a_1$ | — | — |
| $\nu_3{}'$ | — | — |
| $\nu_4(\nu CO)b_2$ | 1590 | X, Y |
| $\nu_4{}'$ | 1612 | Z |
| $\nu_5(\omega CH)b_1$ | ~1364 | X, Y |
| $\nu_5{}'$ | 1383 | X, Y, Z |
| $\nu_6(\rho CH)b_2$ | 1064 | |
| $\nu_6{}'$ | 1064 | X, Z |

\* The $\nu$ and $\nu'$ refer to formate ions I and II respectively.

(ii)  The Internal Fundamentals - $n_i{}'(H_2O)$ *

| Free $H_2O$<br>Fundamental | $n_i{}'(H_2O)$ | Observed<br>Activity |
|---|---|---|
| $\nu_1(\nu OH)a_1$ | ~ 3150 | Y, Z |
| $\nu_2(\delta HOH)a_1$ | 1545 | Z |
| $\nu_3(\nu OH)b_1$ | ~ 3150 | — |

\* As noted in the text $\nu_1(\nu OH)a_1$ is believed to be of higher

frequency than $\nu_3(\nu OH)b_1$.

TABLE 15

## CALCULATED AND OBSERVED INTENSITY RATIOS – $Sr(CHO_2)_2 \cdot 2H_2O$

| Ratios [*] | Calc. | Obs. | Calc. | Obs. | Calc. | Obs. | Product of Obs. Ratios |
|---|---|---|---|---|---|---|---|
| 1 | 0.815 | 0.947 | 0.153 | 0.995 | 0.803 | 0.987 | 0.930 |
| 2 | | 0.907 | | 2.42 | | 0.426 | 0.935 |
| 3 | 1.47 | | 12.3 | | 0.555 | -- | |
| 4 | 1.80 | —— | 0.406 | 0.411 | 1.37 | —— | —— |

[*] 1 – The ratios refer to the combined intensities due to formate ions I and II for both $\nu_2(CHO_2)$ and $\nu_5(CHO_2)$.

2 – The ratios refer to the combined intensities due to formate ions I and II for $\nu_4(CHO_2)$ and water molecules I and II for $\nu_2(H_2O)$.

3 – The ratios refer to the intensities due to formate ions I and II for $\nu_4(CHO_2)$.

4 – The ratios refer to the intensities due to formate ions I and II for $\nu_6(CHO_2)$.

quantitative nature- it was possible to compare observed and calculated intensity ratios in a few cases. These are summarized in Table 15.

## 6-4   Overtones and Combinations of Internal Fundamentals- $Sr(CHO_2)_2.2H_2O$

For $Sr(CHO_2)_2.2H_2O$ we must consider the combinations and overtones of the internal fundamentals $n_i'(CHO_2)$ and $n_i'(H_2O)$. In both cases the discussion of overtones and combinations is completely equivalent to that contained in section 5-4.

From the observed spectra it was possible to make some assignments- these are given in Table 4-1.

## 6-5   Combinations of Internal Fundamentals and Lattice Modes

Reference to Table 12 shows that the lattice vibrations are distributed in the following manner: $(27a, 26b_1, 26b_2, 26b_3)$ If we consider the possible combinations of these lattice modes with the internal fundamentals we find by refering to Table 9 that for internal fundamentals of symmetry species $a, b_1, b_2$ and $b_3$ the respective combination modes possible are: $(27a,26b_1, 26b_2, 26b_3)$, $(27b_1, 26a, 26b_3, 26b_2)$, $(27b_2, 26b_3, 26a, 26b_1)$ and $(27b_3, 26b_2, 26b_1, 26a)$.

Remembering that crystal modes of symmetry species  a are not infrared active the above indicates that for each of

X, Y and Z polarized spectra we would, in principle, expect
the satellite structure of each of the 6 internal fundamental
doublets- $n_i'(CHO_2)$ and each of the 3 internal fundamental
doublets- $n_i'(H_2O)$ to exhibit 210 peaks. Of these 210 peaks
105 will correspond to combination modes and the remaining
105 will correspond to difference modes.

From the observed spectra it was possible to assign
some of the lattice modes. The intense absorptions observed
in the 900-600 $cm^{-1}$ region of the spectrum appear to be
associated with the $_R$ mode observed in the spectrum of ice
and hence can be assigned as lattice modes of rotational
origin ( $\nu_R(H_2O)$ - see Table 4-1). Further tentative
assignments of lattice modes at 18 and 110 $cm^{-1}$ are based on
peak separations between the various internal fundamentals
and the modes associated with their satellite structures.

## CHAPTER VII    CONCLUSIONS

It can be seen from this work that the information obtained from polarized infrared spectra of single crystals can be an important aid in determining crystal structures- this is particularly true where hydrogen atoms or other light atoms are involved.  The factor which most determines the amount and quality of the information obtained from the spectra is the thickness of the crystals.  It would appear that for optimum results- especially where strongly absorbing modes are involved- that the crystal slices should be about 5-10 $\mu$ thick.  This thickness can no doubt be reached as more sophisticated grinding techniques are developed.

This work has shown that the spectra of crystalline materials can be explained on the basis of factor- group analysis.  Future infrared work will, no doubt in part be concerned with attempting to observe the low frequency lattice modes.  Raman Spectroscopy also offers important possibilities in this area.

# BIBLIOGRAPHY

1. K.B. Harvey, B.A. Morrow and H.F. Shurvell,
   Can. J. Chem. 41, 1181 (1963).

2. C.J.H. Schutte and K. Buijs, Spectrochim
   Acta 20, 187 (1964).

3. J.D. Donaldson, J.F. Knifton and S.D. Ross,
   Spectrochim Acta 20, 847 (1964).

4. R. Vierne, Rev. Univ Mines 15, 510 (1959).

5. A.M. Vergnoux and R. Vierne, Comptes Rendus
   261 (6), 1236 (1965).

6. B.A. Morrow, M.Sc. Thesis (U.B.C.), 1962.

7. T.L. Charlton, M.Sc. Thesis (U.B.C.), 1964.

8. I. Nitta, Sci. Papers Inst. Phys Chem. Research
   (Tokyo) 9, 151 (1928).

9. I Nitta and Y. Saito, X-Rays 5, 89 (1949).

10. T. Sugawara, M. Kakudo, Y. Saito and I. Nitta,
    X-Rays 6, 85 (1949).

11. K. Osaki, Ann Rept Sci. Works, Fac. Sci.,
    Osaka Univ. 6, 13 (1958).

12. E. Charney, J.O.S.A. 45, 980 (1955).

13. E.B. Wilson, J.C. Dicius and P.C. Cross,
    Molecular Vibrations, McGraw-Hill (1955).

14. S. Bhagavantam and T. Venkataryudu,
    Theory of Groups and its Application to
    Physical Problems, Andhra University,
    Waltair (1951).

15. R.S. Halford, J. Chem Phys. 14, 8 (1946).